NUMERICAL SIMULATION OF THE SLOSHING OF LIQUIDS IN TANKS

JEFFREY B. SEXTON

NUMERICAL SIMULATION OF THE SLOSHING OF LIQUIDS IN TANKS

BY

© JEFFREY B. SEXTON

A Thesis submitted to the School of Graduate Studies
in partial fulfilment of the requirements for the degree of
Master of Engineering

Faculty of Engineering and Applied Science
Memorial University of Newfoundland

January, 1996

St. John's Newfoundland Canada

ISBN 0-612-13948-4

Abstract

This thesis presents the development and implementation of a Finite Volume Method (FVM) to simulate the sloshing behaviour of incompressible, constant density liquids in a two-dimensional, rigid rectangular tank. The phenomenon of sloshing is of importance to engineers involved in the design of all types of vehicles which transport confined liquids. This paper reports on the research conducted in the context of the transport of liquids on the ocean surface. The method presented has two immediate applications in this context: the transport of petroleum products, and roll stabilization systems for ocean-going vessels.

The FVM is used to discretize the governing momentum and mass conservation equations using primitive variables in a fully Eulerian approach. The method is formulated by integrating the governing equations over appropriate control volumes, and assembling systems of linear equations. A fixed rectangular grid with variable spacing is utilized, and momentum control volumes (CVs) are staggered relative to the continuity CVs. The inertial accelerations caused by a specified tank motion are applied to the fluid by the inclusion of additional source terms in the momentum equations. The method can accommodate the simultaneous translation and rotation of the tank relative to an absolute reference frame, and rotation of the tank about a frame attached to it.

The free surface boundary is handled using the Volume of Fluid (VOF) method, which

permits arbitrary movement of the surface, including the possibility of overlapping and smaller regions breaking away. The VOF method is based on the assignment of a variable F for each continuity CV, where F represents the average fraction of the cell volume which is occupied by fluid. The VOF method, therefore, defines the shape of the fluid-occupied calculation domain, and the free surface.

Results were obtained in the form of the free surface configuration, and velocity and pressure distributions throughout the fluid domain. Results are presented for various prescribed tank motions, chosen to verify the method's stability, reliability, and conformance to behaviour predicted by other established means. Prescribed tank motions were: (i) rotation to a constant angle of inclination; (ii) excitation with the predicted natural period; (iii) excitation near the natural period (producing a surface wave with a "beating" behaviour); (iv) impulsive translation; (v) continuous rotation; and (vi) arbitrary simultaneous rotation and translation. All input tank motions are of a sinusoidal form. The method generated results in good agreement with expected physical behaviour. In particular, the wave period characteristics has been verified, and the ability of the method to accommodate a combined rotational and translational tank motion (representing ship roll and sway) has been proven.

To fully develop and define the capabilities of the proposed method, it is necessary to conduct further testing of the method to verify the surface heights calculated, and to optimize the use of various calculation parameters. In addition, testing with general tank motion (i.e. roll, sway, and heave), and with motions extreme in nature, is recommended. It is also recommended that a version of this method be developed to model a three-dimensional

rectangular tank, thus ensuring its applicability to the widest possible range of practical design problems.

Acknowledgements

I would like to express gratitude to my supervisor, Dr. N. A. Hookey, for his astute guidance and untiring assistance during this research effort, including the process of editing this document. I would also like to thank my family for their support and encouragement in many ways over the course of this work. Specifically, I would like to give recognition to my wife Gail, my two daughters, Jillian and Kayla, and my mother-in-law Emma Thompson, all of whom helped make this possible through their practical support, and understanding.

I must gratefully acknowledge the financial assistance of the Government of Newfoundland, which sponsored this work through an Atlantic Accord Career Development Award. Additional financial support was received from the School of Graduate Studies and the Faculty of Engineering and Applied Sciences at Memorial University of Newfoundland. The use of computer facilities and the assistance of the staff of the Center for Computer-Aided Engineering were also appreciated.

Table of Contents

List of Figures

Nomenclature

Symbol	Description
a	coefficient in discretized form of governing equations
a_x, a_y	acceleration of a fluid particle in the x- and y- directions, respectively
A	upwinding function
b	coefficient of discretized governing equations, incorporating constant terms
C	integrated convective fluid flux across a control volume face
CF	intermediate value in VOF donor-acceptor algorithm
CV	control volume
d, d_c	distance between the free surface and the center of the interpolation neighbour cell, and between continuity CV centers, respectively
D	integrated diffusion fluid flux across a control volume face
ds	differential surface area of a control volume
F	fractional volume of fluid contained in continuity CVs
g	acceleration due to gravity
h	average height of fluid in the tank
$\boldsymbol{h}$	gravity unit directional vector
$\boldsymbol{i}$	unit vector in the x-direction
$\boldsymbol{j}$	unit vector in the y-direction
$\boldsymbol{J}$	convection-diffusion flux vector
J	component of the convection-diffusion flux vector

L	length of tank, measured in x-direction
$\boldsymbol{n}$	unit vector, outward normal to a CV surface ds
o	origin of the (x,y) frame of reference
O	origin of the (X,Y) frame of reference
p	pressure
P	grid Peclet number, or arbitrary point in the (x,y) plane
Q	VOF donor-acceptor algorithm maximum possible volume fluxed across a CV face
$\boldsymbol{R}$	position vector locating an arbitrary point in the moving frame in relation to the fixed frame of reference
$\boldsymbol{r}_1, r_1$	position vector locating the origin of the moving reference frame in relation to the fixed frame, and the length of the vector, respectively
$\boldsymbol{r}_2, r_2$	position vector locating an arbitrary point in the moving frame, and the length of the vector, respectively
$\boldsymbol{S}, S$	source term vector, and its components, respectively
$t, \Delta t$	time, and time step, respectively
T	period of prescribed oscillatory tank motion
$\boldsymbol{U}$	fluid velocity vector
u, v	fluid velocity components, in the x- and y-directions, respectively
$\tilde{u}, \tilde{v}$	updated velocity based on explicit value and pressure gradient, x-direction and y-direction respectively
u^*, v^*	explicit values of velocity, excluding pressure gradient, in x- and y-directions, respectively
$V, \partial V$	volume and surface area of an arbitrary CV, respectively

ΔV	volume of a discretized control volume
x, y	co-ordinates of the moving (tank) reference frame
x_p, y_p	location of an arbitrary point P in the moving frame of reference
X, Y	co-ordinates of the fixed reference frame
$\Delta x, \Delta y$	length of the sides of a rectangular continuity CV, in the x- and y-directions, respectively
$\delta x, \delta y$	distance between main grid nodes, in the x- and y-directions, respectively

Greek Symbols

α	angular acceleration
β	initial angle of inclination
γ	angle of inclination of a point on the grid, measured in the (x, y) frame
ϵ	volume tolerance
η	weight factor for pressure interpolation at surface CVs
θ	instantaneous angle of rotation
μ	dynamic viscosity of the fluid
ρ	mass density of the fluid
Σ	sum of independent variables multiplied by respective coefficients, in the pressure correction equation
ϕ	arbitrarily defined angle combining instantaneous and initial rotation angles
χ, ψ	local surface height function used to determine surface orientation, in the x- and y- direction, respectively
ω	angular velocity

Subscripts

AD	VOF algorithm acceptor or donor cell selector
B	beating wave phenomenon
D	VOF algorithm donor cell indicator
DM	VOF algorithm indicator for cell upstream of the donor cell
E, S, W, N, P	coefficients relating to the east, south, west, north, and center variable in the discretized equation, respectively.
eff	effective
FS	free surface
int	interpolation neighbour CV
i, j	calculation grid index, in the *x*- and *y*-direction, respectively
N	natural period of wave motion
r	relating to a changing position vector
x, y	components in the *x*- and *y*-direction, respectively
θ	relating to rotation
1	fixed reference frame
2	moving reference frame

Superscripts

p	relating to pressure
u, v	relating to the components of velocity in the *x*- and *y*-directions, respectively
n+1	advanced time step level
*	explicit value (of velocity)

Chapter 1

Introduction

1.1 Background

Sloshing exists as a physical phenomenon wherever a confined liquid experiences dynamic forces. A common example of sloshing occurs when a quantity of liquid is being transported, and its container undergoes a motion which is changing, often on a continuous basis and possibly in a random nature. This sloshing motion plays a significant role in the engineering of transport vehicles, whether the mode of travel is by land, air, water, or even outside the influence of the earth's atmosphere. The reaction forces generated on a container by a sloshing fluid are often greater than the static forces, and may be greater than reaction forces determined by assuming an effectively rigid cargo on an accelerating vehicle. The reaction forces found due to sloshing may also be in or out of phase with the vehicle accelerations. The magnitude and phase of the reaction forces can contribute to vehicle instability, while the phase relationship between the reaction forces and the vehicle motion may increase the physical stability of the vehicle. The reaction forces, and the corresponding moments, must, therefore, be taken into account in the design of the container and the transporting vehicle.

The analysis of sloshing behaviour first gained significant attention in the 1950s, when the influence of the inertia of sloshing fuel was seen upon the trajectory of rockets. This led to major research efforts into sloshing in micro gravity environments. A more down-to-earth

example of sloshing and its effect on public safety is in the transport of liquids by road container, where the dynamic stability of a tanker truck can be significantly affected by sloshing.

The importance of sloshing in ship tanks has long been known, and is particularly relevant to cases in which ships operate with partly-filled tanks for significant periods of time, or during occasions when extreme loading conditions may occur. The relevance of sloshing to the design and operation of a particular ship depends entirely upon the type of ship, its cargo, service, and the geographic region in which it operates. For instance, while most ocean-going tankers normally travel with full holds (largely for economic reasons), there are instances when travel with a partly-full hold is unavoidable. Floating production, storage and off-loading (FPSO) vessels operate in such a way that sloshing is a very important consideration for stability. Hamlin et al. [1] give a comprehensive discussion of sloshing in ships, and present extensive test results and specific case applications. Both R.L. Bass et al. [2] and Tanaka et al. [3] report on a considerable amount of work that has been done regarding the design and operation of liquefied natural gas (LNG) carriers in particular. For many types of ships, however, roll stabilization has been achieved using a dedicated and purpose-designed slosh tank with the out-of-phase motion of the liquid contents used to enhance the seakeeping capabilities of the vessels. References [4] and [5] provide considerable insight into this area of marine vessel design.

The motivation of the author stems from experience in the design of structural supports for mechanical equipment being transported at sea, and participation in the layout of a service barge for a marine construction project. In the latter instance, a fuel system for temporary

and emergency electric power generation was designed for the barge, including the use of fuel storage tanks. The design of the barge general arrangement and equipment support necessarily took into account an extreme condition wave-induced barge motion. The most direct application of the research presented in this thesis is as a tool in the design of rectangular (i.e. simple-shaped) petroleum containers, typical of those used to store jet fuel on fixed offshore production platforms. These containers are transported to remote offshore sites on the decks of supply vessels, and they can experience highly varying forces.

The study of sloshing has been undertaken by many people over the last four decades, and a variety of approaches have been used. Theoretical investigations of the mathematical equations governing liquid motions in free surface problems have led to a high degree of understanding of their meaning. Linearized wave theory has effectively been applied to sloshing in an enclosed boundary (no inflow or outflow) to allow prediction of natural frequencies of cyclic surface wave motion. Potential flow theory has been used to study the wave motion of ideal fluid flows, including sloshing in rectangular tanks [6]. Analytical solutions of viscous flows for physical configurations that occur in real applications are virtually impossible to obtain.

Many experimental studies of sloshing have also been performed. To conduct a comprehensive experimental study is often costly (in material and time), limited by physical constraints, and may often involve safety risks. Design processes are advanced by the development of empirical relationships and formulae based on physical testing, however, and experiments are the only means of determining the real behaviour of a sloshing fluid in a given application.

A third approach in study and analysis is numerical modelling. This field of endeavour has grown and developed steadily, with techniques evolving and computer capabilities increasing, to the point where a variety of techniques have been applied to many configurations of the free surface fluid problem. Numerical modelling, along with theoretical background, allows a detailed study of sloshing, with the possibility of detailed information on the effects of sloshing. Methods must be based on sound theory, and validated against experimental data, and can then be used to advance the design process, both to enable one to prescribe model tests efficiently, and as input to final designs.

1.2 Aims and Motivations of the Thesis

The aim of this research is to develop a method suitable for the simulation of the two-dimensional sloshing of a viscous fluid contained in a tank that has been given a known motion. To achieve this goal, the method must satisfy the following requirements:

(1) A time-domain approach using primitive variables was desired. This would allow the specification of input velocities, accelerations, and forces in a direct manner, and the output would be fluid velocities, accelerations, and pressures. The forces and moments acting upon the container may be directly calculated from this data.

(2) The method must be capable of handling arbitrary liquid motions, and hence relatively large motions, to ensure applicability to various real design problems.

(3) The method must be suitable for extension to three-dimensional formulations, to allow for application to more complex design problems. The current work is in two

dimensions only.

(4) A pre-disposition was held towards a method based on the Finite Volume Method (FVM) of deriving the discretized equations. The FVM is well suited to the simulation of fluid flow problems, and it aids the physical interpretation of results.

1.3 Literature Survey

A survey of the literature relating to numerical methods applied to sloshing problems showed that many of the methods being used have had their basis in methods developed to deal with fluid problems which may be considered more basic, or in some instances, are unique cases of a free surface problem. Indeed, even some of the more recently-developed efforts are presented in the context of unique or fundamental cases. Many methods are, however, presented as being applicable to several forms of the free surface problem. The objectives of this survey were: (i) to get a general overview of the types of approaches that have been used to date; (ii) to become familiar with how some of these approaches have been modified over time; and (iii) to select an approach to modelling the sloshing problem for this research project.

The literature indicates that methods have been developed based on either or both of the Eulerian and Lagrangian views of the free surface problem. In Eulerian methods the mesh in the calculation domain is fixed, and the fluid occupies parts of the mesh. The principal problem is to determine which parts of the mesh are occupied by fluid at any point in time. In Lagrangian methods, the mesh moves with the fluid, such that the edges of the mesh define the fluid domain. The main task in these methods is to deform the mesh in accordance with

the motion of the fluid. The following two sub-sections discuss methods based on the Eulerian and Lagrangian approaches, respectively.

1.3.1 Eulerian Methods

The development of methods using the Eulerian approach to free surface problems was spearheaded by the Los Alamos Scientific Laboratory of the University of California. Harlow and Welch published their landmark paper on the Marker and Cell (MAC) technique in 1965 [7]. The MAC method employs "markers" to track and move the free surface through the Eulerian grid of calculation cells. The location of these fictitious marker particles are defined at the beginning of the calculation, and their location is continuously updated at each time step. The original MAC method used a finite difference (FD) discretization of the Navier-Stokes equations, applied to incompressible viscous flows. This paper was also the first application of staggered grids to primitive variable fluid flow problems. The boundary condition of tangential stress at the surface is achieved by enforcing divergence of velocity equal to zero at the free surface. Boundary conditions for both the free surface and solid boundaries are established by the specification of fictitious velocity nodes outside the actual boundary location. The paper presented the simulation of the collapse of a dam, and the opening of a sluice gate as example problems.

There have been several efforts made to apply the MAC method to other free surface problems, several based upon, or resulting in, modifications to the original method. Among them Viecelli's 1969 paper [8] provided an improved procedure for including boundary conditions which allowed the handling of arbitrarily-shaped boundaries, whether solid or free surface. The procedure is based upon adjustment of pressure in a given cell to achieve the

desired flow at the boundary. Viecelli's two-dimensional examples were a liquid column falling (i) into a circular tank, and (ii) past a circular obstacle in a vertical channel. Nichols and Hirt [9] proposed improvements to free surface boundary conditions which consisted of specifying pressure at a surface cell center based upon an interpolation of the pressure at the center of a neighbouring cell, and normal stresses, if the latter were to be specified for a particular problem. This calculation required the assessment of the orientation of the surface within a surface cell, using the marker particles defining the surface. The sample problems simulated by Nichols and Hirt [9] include the collapse of a fluid column, a rotating column of fluid, a drop splashing into a deep pool, and a viscous bore. Amsden and Harlow [10] presented a simplified method (SMAC) which attempted to deal with aspects of MAC which the authors state were complicated. These aspects were: (i) the application of boundary conditions for obstacles and inflow/outflow boundaries; and (ii) the solution of the Poisson equation for any but the most simple configurations. The simplification of the calculation technique was achieved using vorticity and a potential function to correct the velocity field and hence satisfy the continuity requirement without calculating pressures explicitly. Example problems in [10] are the collapsing column of fluid, waterfall over a step, reservoir flow-through, flow over a step, and flow past a scow. Chan and Street [11] presented Stanford University's Modified MAC method of modelling water waves (SUMMAC), which omits the viscous terms, but makes the following improvements in finite difference calculations: (i) rigorous application of the pressure boundary condition at the free surface; and (ii) extrapolation of velocity components from the interior to enable more accurate shifting of the free surface boundary. Further, a second-order explicit difference scheme was used for the calculation of the convective flux terms, as compared to the first-order scheme in the original MAC version. To promote greater stability for long-term calculations, a forward implicit

scheme was implemented in SUMMAC for the advancement of marker particles. The case studies presented deal with waves encountering a sloping beach.

The MAC methods employ the marker particles either throughout the fluid, or only in the surface cells, the latter resulting in a "string" of particles defining the location of the surface boundary. In the latter approach, one can define the surface either by a set of points connected by ordered line segments, or one can represent the surface by a single-valued height function (i.e. $h = h(x, t)$, where h is the fluid height above the bottom of a stationary two-dimensional grid). These schemes are simple to apply only when the surface remains nearly horizontal, and neighbouring particles remain connected in the same sequence throughout the process. To accommodate multi-valued surfaces (i.e. bubbles), parts of the fluid breaking away, repeated changing from horizontal to vertical orientations, or the surface folding back upon itself, considerable accounting and adjusting is required with these two schemes, rendering the understanding and programming of them tedious. In fact, in principle, a height function cannot be used to model a bubble. The major advantage of the use of a string of particles for suitable problems, however, is that less data storage is required, in comparison to the approach of marker particles imbedded throughout the fluid-occupied domain.

When the MAC method employs particles imbedded through all of the fluid cells, the movement of the particles is a Lagrangian device used to define the spatial regions occupied by the fluid, and this knowledge is used to perform the flux calculations in an Eulerian mesh. The precise location of the free surface boundary requires an additional computation, based on marker distribution. To enforce the surface boundary condition may require the use of one

of the methods described above for surface tracking. A limitation inherent in these MAC methods is that the markers can be transported out of the fluid domain, and one must continuously replace them. Also, markers may be concentrated in narrow regions of the domain, requiring the addition or deletion of markers to provide a suitable approximation to the free surface.

In 1975 Nichols et al. [12] published a report on the SOLA method, which is a simplified version of the MAC technique for confined flows (no free surface); SOLA (SOLution Algorithm) does not use marker particles, and is not set up for internal obstacles. To simulate free surface flows, Nichols et al. [13,14] developed the Volume of Fluid (VOF) method, used in conjunction with SOLA. The VOF method offers the advantages of defining and monitoring fluid regions in order to move fluid through the Eulerian grid, without the disadvantages of having to define and monitor particle movement. It allows the possibility of multi-valued or discontinuous free surface interfaces, while avoiding the large storage and computing time required to monitor particle movement. The VOF method assigns a value to a variable F for each cell, where an F value of zero means a cell is empty, a value of one means it is full, and an intermediate value indicates that the cell contains a free surface. A donor-acceptor algorithm was developed to allow convecting the fluid from one cell to another, thus allowing the surface to move through the Eulerian grid. The problem reduces to solving for the distribution of F throughout the calculation domain, and thereby defining the portion of the Eulerian mesh occupied by fluid. The SOLA-VOF method presented in [13,14] can handle irregular surface motions, Cartesian and polar cylindrical co-ordinate systems, variable mesh spacings, obstacles, multi-fluid interfaces, and limited compressibility. This method is a finite difference technique specifying pressure on the free surface boundary

by interpolation of the value at a neighbour cell, and setting velocity boundary conditions via fictitious values outside the boundary. The versatility of SOLA-VOF was demonstrated in [13,14] by application to the simulation of a breaking bore, the broken dam problem, the collapse of a cylindrical column of fluid, perturbation of a thin cylindrical fluid column, extrusion of an immiscible droplet, and gas bubble ejection from a submerged vent pipe.

Other authors have applied the VOF technique to tank sloshing similar to the configuration of interest in this research. Bridges [15] modelled sloshing of liquid in a rectangular container, and presented results of experiments for comparison. Bridges' approach was to use a SOLA-VOF model (two-dimensional), with all motions defined in relation to the tank itself; rotational motion of the tank was introduced as accelerations experienced by the liquid in the tank. Su and Kang [16] employed the SOLA-VOF method with an improvement made in the flux transfer calculation of the donor-acceptor algorithm. In [16] the two-dimensional sloshing in a tank undergoing a forced sinusoidal sway was simulated and compared to experimental data. Su [17] also reports numerical results for many baffled and unbaffled two-dimensional tank configurations, and compares the influence of different baffle arrangements and tank aspect ratios on the reaction forces. These numerical calculations had also been done by T. J. Bridges using a VOF method. The details of the method used in [17] were not discussed.

Several other researchers have reported on the use of variations in the MAC method for sloshing problems. For example, Arai [18] modelled two-dimensional rectangular tanks with baffles using the MAC method (inviscid fluid), giving the tank oscillatory pitching motion. Physical experiments were also performed, and the results of numerical and physical tests

were compared for a pitching amplitude of 2 degrees. Cordonnier [19] employs TUMMAC (Tokyo University Modified-MAC) to perform two-dimensional numerical studies, and compares these to experiments with a rectangular tank. Information on how MAC is modified in this method were not given. Japan-based researchers Arai et al. [20] used a MAC-based three-dimensional model, incorporating solution techniques of SOLA, and applying the method to the analysis of FPSO vessels. Results of experiments were also given. Popov and others at Concordia have used SOLA to model sloshing in two-dimensional rectangular tanks [21,22] and horizontal cylinders [23], in the context of road transportation of liquids.

The VOF method has also been used to address research into other free surface problems. For instance, Abdullah and Salcudean [24] apply the VOF method to the turbulent filling of a cylinder. Partom [25] applied the VOF algorithm to a three-dimensional problem involving the motion of a wall of fluid in a partially-filled horizontal cylindrical container.

1.3.2 Lagrangian Methods

Considerable work has also been done on Lagrangian numerical methods for the simulation of free surface flows, where it is necessary to move the computational mesh with the moving fluid. More sophisticated methods which can accommodate either or both of Lagrangian and Eulerian calculations in a combination have also been developed. The latter are usually labelled as Arbitrary Lagrangian-Eulerian (ALE) methods. In pure Lagrangian methods the mesh moves with the fluid such that a nodal point would follow a particular fluid particle path; this can lead to significant problems with mesh contraction and concentration. Also, Lagrangian methods may require deletion or addition of nodes to provide sufficient nodes for

continued discretization of the problem. Lagrangian methods suffer significant penalties with regard to gridding. In ALE methods, the grid is not necessarily moved with the fluid. For example, a node does not necessarily move with the concurrent fluid particle, but may move only a portion of the displacement of the particle. This helps to reduce meshing problems, but results in more complicated discretization methods required to determine the appropriate diffusion and convection terms to be used for cells of changing size and/or orientation.

In these areas of research, Finite Element Methods (FEMs) have generally dominated due to geometry considerations. The published literature includes Huerta and Liu [26], who developed a two-dimensional ALE Petrov-Galerkin FEM. The problems studied in [26] were the impact of tsunamis on a continental shelf, dam breaking, and sloshing in a rectangular container. Ramaswamy and Kawahara developed a Lagrangian Galerkin FEM [27], and further an ALE formulation [28], to examine several two-dimensional test problems, including sloshing in a prismatic container. Ramaswamy and Kawahara [29] used a Lagrangian FEM formulation, along with velocity correction borrowed from FD methods, to model two-dimensional sloshing in a rectangular container. The forcing motion utilized was sinusoidal pitching, with an angle amplitude of 0.2 degrees.

The ALE methods, while attempting to deal with large motions of fluid surfaces, require arbitrary control of how and under what conditions the grid is to be re-meshed. This control can only be achieved by trial-and-error, and/or a prior knowledge of how the fluid will respond to the forces it experiences. There does not appear to be any recorded means of accommodating discontinuous surface segments in the FEMs discussed in this literature survey.

1.3.3 Summary

The review of available literature reveals that Eulerian methods offer distinctly attractive features for the numerical modelling of free surface fluid motions in a partly-filled container. The main advantage of methods which take the Eulerian viewpoint is that the surface is permitted free movement according to its governing physical laws, and its configuration can be monitored, without restriction on its shape or continuity. Among Eulerian methods, the Volume of Fluid method was found to offer the capability to achieve this in the simplest and most efficient manner. In particular, the VOF approach offers the ability to handle relatively large fluid motions, discontinuous surface segments, multi-valued surfaces, and the surface collapsing upon itself. This has enabled the development of methods with the potential to simulate such behaviour as wave breaking and impacts on tank top covers, as well as large wave heights. It should be noted, however, that in all of the methods applying the VOF technique to sloshing, the specified tank motion has been restricted to either rotation or translation; none have allowed a combination of both of these types of motion.

1.4 Definition of Research

The objectives of this research effort are to gain an understanding of both the physical behaviour of the sloshing of liquids in rigid containers, and the numerical modelling of such problems. Specifically, the goals of the numerical model development were as follows:

(1) Develop a two-dimensional FVM-based numerical procedure to calculate the motion characteristics of an incompressible viscous liquid in a partially-filled rigid rectangular container. The free surface will be handled by the application of the Volume of Fluid

method.

(2) Incorporate into the method the ability to specify a tank motion of any combination of translation and rotation.

(3) Verify the model against relevant theory, and available experimental and numerical data.

(4) Demonstrate the ability of the model to predict fluid motions, and calculate local fluid pressures, for physically realistic tank motions.

Chapter 2

Method

The formulation of a FVM for unsteady, viscous, incompressible fluid flows with a free surface is presented in this chapter. The following topics are each addressed in a section: (1) definition of the governing equations; (2) kinematics of the problem; (3) discretization of the fluid domain; (4) integral conservation equations; (5) derivation of the discretized form of the governing equations; (6) treatment of the boundary conditions for the free surface and solid boundaries; and (7) the algorithms used to solve the discretized equations. A summary of the method is presented in the final section of the chapter.

2.1 Governing Equations

The equations governing the unsteady, two-dimensional motion of an incompressible, viscous fluid are the Navier-Stokes equation

$$\rho \frac{\partial \boldsymbol{U}}{\partial t} + \rho(\boldsymbol{U}\cdot\nabla)\,\boldsymbol{U} = -\rho g \nabla \boldsymbol{h} - \nabla p + \mu\,\nabla^2 \boldsymbol{U} \qquad (2\text{-}1)$$

and the continuity equation

$$\nabla\cdot\boldsymbol{U} = 0 \qquad 60(2\text{-}2)$$

where $\boldsymbol{U}$ is the velocity vector of the fluid, g is the body force acceleration (gravity), $\boldsymbol{h}$ is the

gravity directional unit vector, p is the pressure, ρ is the mass density of the fluid (which has been assumed constant), μ is the dynamic viscosity of the fluid, and t is time.

The governing equations are solved using the Cartesian co-ordinate system (x,y) attached to the container as shown in Figure 2-1. To produce sloshing, the tank is caused to move relative to a fixed co-ordinate frame (X,Y). The motion of the tank produces inertial forces on a fluid particle and this results in additional acceleration terms to be included in the governing momentum equations. These additional terms are described in section 2.2. When the terms are included in the Navier-Stokes equation, the x-component of equation (2-1) can be written in the following compact form:

$$\rho \frac{\partial u}{\partial t} + \nabla \cdot \boldsymbol{J}^u = S^u - \frac{\partial p}{\partial x} \tag{2-3}$$

where $\boldsymbol{J}^u$ is the convection diffusion flux vector, and S^u is a source term. The source term will incorporate body forces (gravity) and inertial forces caused by the tank motion. Using the results of section 2.2, $\boldsymbol{J}^u$ and S^u are defined as follows:

$$\boldsymbol{J}^u = \rho \boldsymbol{U} u - \mu \nabla u \,, \tag{2-4}$$

$$\begin{aligned} S^u = -\rho g_x - \rho \Big[& \ddot{r}_1 \cos\phi_1 - 2\dot{r}_1 \omega_1 \sin\phi_1 - \omega_1^2 (r_1 \cos\phi_1 + x_p) \\ & - \alpha_1 (r_1 \sin\phi_1 + y_p) - 2v\omega_1 - \alpha_2 y_p - \omega_2^2 x_p - 2v\omega_2 \Big] \end{aligned} \tag{2-5}$$

Equation (2-3) can represent the y-momentum equation when v replaces u in the unsteady term, and $\boldsymbol{J}^u$, S^u and $\partial p/\partial x$ are replaced by $\boldsymbol{J}^v$, S^v and $\partial p/\partial y$, respectively, where $\boldsymbol{J}^v$ and

S^v are defined as follows:

$$J^v = \rho U v - \mu \nabla v \,, \tag{2-6}$$

$$S^v = -\rho g_y - \rho\Big[\ddot{r}_1 \sin\phi_1 + 2\dot{r}_1\omega_1 \cos\phi_1 - \omega_1^2(r_1 \sin\phi_1 + y_p) + \alpha_1(r_1 \cos\phi_1 + x_p) + 2u\omega_1 + \alpha_2 x_p - \omega_2^2 y_p + 2u\omega_2\Big] \tag{2-7}$$

In equations (2-5) and (2-7) the g_x and g_y terms are the x and y components of the gravitational acceleration respectively, which are defined as follows:

$$g_x = g \sin(\beta_2 + \phi_2) \tag{2-8}$$

$$g_y = g \cos(\beta_2 + \phi_2) \tag{2-9}$$

where

$$\phi_2 = \theta_1 + \theta_2 \tag{2-10}$$

as shown in Figure 2-1. The remaining terms in equations (2-5) and (2-7) are fully described in the following section.

2.2 Kinematic Relationships

In this thesis the two-dimensional sloshing of a liquid in a moving container is simulated by solving the governing equations using an Eulerian method which employs calculation mesh that is fixed to the moving tank. As illustrated in Figure 2-1, the Cartesian co-ordinate system (x, y) is attached to the moving tank. The tank can have an initial angle of inclination to the

horizontal of β_2. The tank (and the (x, y) frame) may rotate about the origin of the (x, y) frame, o, with angular displacement, velocity, acceleration of θ_2, ω_2, and α_2, respectively. The location of a point P in the calculation mesh fixed to the tank can be referenced to the origin of the (x, y) frame by the vector $\boldsymbol{r}_2$ which is at an angle γ to the x-axis. The magnitude and direction of $\boldsymbol{r}_2$, with respect to the (x, y) frame, remain fixed during the tank motion.

The position of the origin of the (x, y) frame is located in a global, or fixed, frame of reference (X,Y) by the vector $\boldsymbol{r}_1$. The position vector $\boldsymbol{r}_1$ may have an initial angle of inclination to horizontal (i.e. the X axis) of β_1. To allow for motion of the tank relative to the fixed frame, $\boldsymbol{r}_1$ is permitted to rotate about origin O with angular displacement, velocity, and acceleration of θ_1, ω_1, and α_1, respectively, and it is permitted to change length with velocity and acceleration of $\dot{r}_1$, and $\ddot{r}_1$, respectively. This method, therefore, allows the specification of truly arbitrary tank motion. Previous methods (e.g. [15,16,18,20]) have allowed only rotation and/or translation in relation to the (X,Y) frame, whereas this research allows the rotation of the (x, y) about its origin to be included as well.

The motion of the tank will lead to the generation of several terms which must be appropriately accounted for when determining the acceleration of a fluid particle at a point P in the mesh at any instant in time. These additional terms must also be resolved into components in the (x, y) frame, as the governing equations are solved in this co-ordinate system. Defining the following co-ordinates of point P:

$$x_p = r_2 \cos\gamma \tag{2-11}$$

$$y_p = r_2 \sin\gamma \tag{2-12}$$

and the angle:

$$\phi_1 = \beta_1 - \beta_2 - \theta_2 \tag{2-13}$$

the x- and y- components of the acceleration of a fluid particle located at point P, at a given instant in time, may be written as follows:

$$\begin{aligned} a_x = \frac{Du}{Dt} &+ \ddot{r}_1\cos\phi_1 - \omega_1^2(r_1\cos\phi_1 + x_p) - \alpha_1(r_1\sin\phi_1 + y_p) \\ &- 2\dot{r}_1\omega_1\sin\phi_1 - 2v\omega_1 - \omega_2^2 x_p - \alpha_2 y_p - 2v\omega_2 \end{aligned} \tag{2-14}$$

$$\begin{aligned} a_y = \frac{Dv}{Dt} &+ \ddot{r}_1\sin\phi_1 - \omega_1^2(r_1\sin\phi_1 + y_p) + \alpha_1(r_1\cos\phi_1 + x_p) \\ &+ 2\omega_1\dot{r}_1\cos\phi_1 + 2u\omega_1 - \omega_2^2 y_p + \alpha_2 x_p + 2u\omega_2 \end{aligned} \tag{2-15}$$

In equations (2-14) and (2-15) the first term is the total derivative defining the acceleration of a fluid particle at point P in the (x, y) frame. The second through sixth terms are due to the rotation and translation of the (x, y) frame relative to the (X,Y) frame. The remaining three terms are due to the rotation of (x, y) about its origin. The second term is due to the translational acceleration of frame (x, y) relative to the absolute reference frame. The third and fourth terms are the normal and tangential acceleration terms due to the rotation of the tank about the origin of the (X,Y) frame. The fifth and sixth terms are Coriolis accelerations due to the rotation and translation of the (x, y) frame about the origin of (X,Y), and the

rotation of a fluid particle with velocity $\boldsymbol{U}$ at point P about (X,Y) with angular velocity ω_1, respectively. The seventh and eighth terms are the normal and tangential acceleration terms, respectively, at P due to the rotation of the (x, y) frame about its origin. The final term is the Coriolis acceleration experienced by the moving fluid particle at point P, due to the rotation of the (x, y) frame about its origin.

When the accelerations given by equations (2-14) and (2-15) are substituted into the appropriate governing equations, the extra acceleration terms may be included in source terms, as shown in equations (2-5) and (2-7). The actual accelerations terms that would be present for a particular problem would depend upon the nature of the prescribed motion.

2.3 Discretization of the Domain

The governing equations are discretized using the finite volume approach, as described by Patankar [30]. A staggered mesh, where pressure and velocity components are stored at different locations, is used to prevent oscillatory solution fields. In this method, the calculation domain is discretized with rectangular control volumes (CVs), as outlined by the dashed lines in Figure 2-2 . In this figure, i and j are indices in the x and y directions, respectively, and the dimensions of a main grid CV are defined as Δx_i and Δy_j. Following Patankar's Practice B, the main grid nodes are then placed at the geometric center of the main grid CVs, and the distances between nodes are defined as δx_i and δy_j.

The values of pressure, density, and viscosity are stored at the main grid nodes, while the values of velocity (u and v) are stored at the center of the control volume faces to which

they are normal. This results in the staggered storage arrangement shown in Figure 2-3, where the v - CV is typical of those on the south and north boundaries of the domain, and the u - CV is typical of internal CVs (i.e. u - CVs on the west and east boundaries are similar to the v - CV shown).

The discretized forms of the governing equations are obtained by integrating them over a control volume, with the assumption that the fluxes across a CV face are uniform. Different control volumes are utilized for each of the equations. The staggered momentum CVs are chosen such that the velocity value under consideration is centered in, or best represents the mean value for, the control volume.

2.4 Integral Conservation Equations

In the finite volume method used in this thesis, the Navier-Stokes equations are integrated over the discrete control volumes in the calculation domain and over a time interval. Using Gauss' divergence theorem, the integration of equation (2-3) over a control volume V that is fixed relative to the (x,y) frame, and over a time interval Δt, results in the following integral conservation equation for x-momentum:

$$\rho \int_t^{t+\Delta t} \int_V \frac{\partial u}{\partial t} dV dt + \int_t^{t+\Delta t} \int_{\partial V} \boldsymbol{J}^u \cdot \boldsymbol{n} \, ds \, dt = \int_t^{t+\Delta t} \int_V S^u dV dt - \int_t^{t+\Delta t} \int_V \frac{\partial p}{\partial x} dV dt \qquad (2\text{-}16)$$

where ∂V is the surface of the CV, and $\boldsymbol{n}$ is the unit outward normal to the differential surface area ds. A similar integral conservation equation may be obtained for y-momentum. The

continuity equation is also integrated over a control volume to give the following integral conservation equation:

$$\int_{\partial V} \boldsymbol{U} \cdot \boldsymbol{n}\, ds = 0 \tag{2-17}$$

2.5 Derivation of the Discretized Equations

To obtain algebraic approximations of the integral conservation equations for the appropriate control volume, approximations to the contributions of each CV must be derived and assembled in a suitable manner. The derivation of the discretized forms of the x- and y-momentum, and the continuity equations will be discussed in this section.

2.5.1 Momentum Equations

2.5.1.1 x - momentum

The convection diffusion flux in the integral conservation form of the x-momentum, equation (2-16), can be separated into components in the x and y directions as follows:

$$\boldsymbol{J}^u = J_x^u \boldsymbol{i} + J_y^u \boldsymbol{j} \tag{2-18}$$

where

$$J_x^u = \rho u(u) - \mu \frac{\partial u}{\partial x}, \tag{2-19}$$

$$J_y^u = \rho v(u) - \mu \frac{\partial u}{\partial y}, \tag{2-20}$$

and $\boldsymbol{i}$ and $\boldsymbol{j}$ are the unit vectors in the x- and y- directions, respectively.

To integrate these fluxes over the surface of the x - momentum CV (see Figure 2-3), the fluxes are assumed constant over a face, and are evaluated using a power law scheme, as described by Patankar [30]. The source term in equation (2-5) is assumed to be constant over the control volume, and the equation is integrated explicitly in time. The resulting form of the discretized x-momentum equation can be written as follows:

$$u_P^{n+1} = \left[b^u + a_P^u u_P + a_N^u u_N + a_E^u u_E + a_S^u u_S + a_W^u u_W \right] \frac{\Delta t}{\rho \Delta V^u} + (p_{i-1,J} - p_{i,J}) \frac{\Delta t}{\rho \delta x_i} \qquad (2\text{-}21)$$

The variable u_P represents the velocity at node i,j. The superscript $n+1$ on velocity means the next time step value, whereas all terms without this superscript are evaluated at the current time value. The value u_N is the neighbouring u-value to the north of the point being considered (i.e. $u_{i,j+1}$), the variable u_E represents the value to the east (i.e. $u_{i+1,j}$), and so on for the four neighbouring u values. The variables a^u_N is the coefficient multiplying the east neighbour. Similarly, a^u_E, a^u_S, and a^u_W are the coefficients multiplying the east, south, and west neighbours respectively; a^u_P is the center point coefficient. The pressures $p_{i-1,j}$ and $p_{i,j}$ are those on the west and east CV faces for u_P, and Δt is the time interval. The variable ΔV^u is the volume of the CV; taking the third dimension as a unity value, this value is effectively the area of the CV for a two-dimensional problem. The b^u term is a constant incorporating the body force term and appropriate terms from the kinematics of the tank motion. The coefficients in equation (2-21) are defined as follows, in accordance with Patankar [30]:

$$a_N^u = D_n A(|P_n|) + [\![-C_n, 0]\!] \qquad (2\text{-}22a)$$

$$a_S^u = D_s A(|P_s|) + [\![C_s, 0]\!] \qquad (2\text{-}22b)$$

$$a_E^u = D_e A(|P_e|) + [\![-C_e, 0]\!] \qquad (2\text{-}22c)$$

$$a_W^u = D_w A(|P_w|) + [\![C_w, 0]\!] \tag{2-22d}$$

$$a_P^u = \frac{\rho \Delta V^u}{\Delta t} - a_N^u - a_E^u - a_S^u - a_W^u \tag{2-22e}$$

$$b^u = S^u \Delta V^u \tag{2-22f}$$

where the double square brackets mean the greater of the quantities contained within them. The D terms represent the integrated diffusion flux over a face, and the C terms are the integrated convection flux across a given face. These are determined as follows:

$$D_n = \mu_n \delta x_i / \delta y_{j+1} \qquad C_n = \rho v_n \delta x_i \tag{2-23a}$$

$$D_s = \mu_s \delta x_i / \delta y_j \qquad C_s = \rho v_s \delta x_i \tag{2-23b}$$

$$D_e = \mu_e \Delta y_j / \Delta x_i \qquad C_e = \rho u_e \Delta y_j \tag{2-23c}$$

$$D_w = \mu_w \Delta y_j / \Delta x_{i-1} \qquad C_w = \rho u_w \Delta y_j \tag{2-23d}$$

Defining the grid Peclet numbers,

$$P_n = C_n / D_n \tag{2-24a}$$

$$P_s = C_s / D_s \tag{2-24b}$$

$$P_e = C_e / D_e \tag{2-24c}$$

$$P_w = C_w / D_w \tag{2-24d}$$

allow the function $A(|P|)$ for the Power Law scheme [30] to be specified as follows:

$$A(|P|) = [\![0, (1 - 0.1|P|)^5]\!] \tag{2-25}$$

2.5.1.2 y - momentum

The approach taken in the discretization of the x - momentum is also used to discretize the y-momentum equation; the integration is performed on the v-velocity CV, as shown in Figure

2-3. The flux terms are defined as follows:

$$\boldsymbol{J}^{v} = J_x^{v}\boldsymbol{i} + J_y^{v}\boldsymbol{j} \tag{2-26}$$

where the components are:

$$J_x^{v} = \rho u(v) - \mu\frac{\partial v}{\partial x} \tag{2-27}$$

$$J_y^{v} = \rho v(v) - \mu\frac{\partial v}{\partial y} \tag{2-28}$$

Integrating the fluxes over the CV surface results in the following expression for the updated v-velocity value at point i,j :

$$v_P^{n+1} = \left[b^{v} + a_P^{v}v_P + a_N^{v}v_N + a_E^{v}v_E + a_S^{v}v_S + a_W^{v}v_W\right]\frac{\Delta t}{\rho\Delta V^{v}} + (p_{i,j-1} - p_{i,j})\frac{\Delta t}{\rho\delta y_j} \tag{2-29}$$

In equation (2-29) the coefficients and variables are analogous to those defined for equation (2-21). The coefficients are evaluated as follows:

$$a_N^{v} = D_n A(|P_n|) + [\![-C_n, 0]\!] \tag{2-30a}$$

$$a_S^{v} = D_s A(|P_s|) + [\![C_s, 0]\!] \tag{2-30b}$$

$$a_E^{v} = D_e A(|P_e|) + [\![-C_e, 0]\!] \tag{2-30c}$$

$$a_W^{v} = D_w A(|P_w|) + [\![C_w, 0]\!] \tag{2-30d}$$

$$a_P^{v} = \frac{\rho\Delta V^{v}}{\Delta t} - a_N^{v} - a_E^{v} - a_S^{v} - a_W^{v} \tag{2-30e}$$

$$b^{v} = S^{v}\Delta V^{v} \tag{2-30f}$$

and the integrated fluxes are determined by:

$$D_n = \mu_n \Delta x_i / \Delta y_j \qquad C_n = \rho v_n \Delta x_i \tag{2-31a}$$

$$D_s = \mu_s \Delta x_i / \Delta y_{j-1} \qquad C_s = \rho v_s \Delta x_i \tag{2-31b}$$

$$D_e = \mu_e \delta y_j / \delta x_{i+1} \qquad C_e = \rho u_e \delta y_j \tag{2-31c}$$

$$D_w = \mu_w \delta y_j / \delta x_i \qquad C_w = \rho u_w \delta y_j . \tag{2-31d}$$

The grid Peclet numbers are found using equations (2-24), and the $A(|P|)$ function is defined in equation (2-25).

2.5.2 Continuity

The explicit equations for the velocities, equations (2-21) and (2-29), will yield values for the advanced time step, but the new values will not in general satisfy continuity, since pressure values used are those valid for the previous time level. Hence, what is really needed is u, v, and p solved simultaneously for the advanced time level. This thesis uses a method of discretizing the continuity equation which is similar to the method proposed by Hirt and Nichols [13] in their SOLA method. In this method, the pressure at the advanced time level, $p^{n+1}_{i,j}$, is defined as the previous time level value plus a pressure correction δp:

$$p^{n+1}_{i,j} = p_{i,j} + \delta p_{i,j} \tag{2-32}$$

If equation (2-32) is substituted into equations (2-21) and (2-29), the following expressions can be obtained:

$$u^{n+1}_p = \tilde{u}_p + (\delta p_{i-1,j} - \delta p_{i,j}) \frac{\Delta t}{\rho \delta x_i} \tag{2-33}$$

$$v^{n+1}_p = \tilde{v}_p + (\delta p_{i,j-1} - \delta p_{i,j}) \frac{\Delta t}{\rho \delta y_j} \tag{2-34}$$

where

$$\tilde{u}_P = u_p^* + (p_{i-1,j} - p_{i,j}) \frac{\Delta t}{\rho \delta x_i} \tag{2-35}$$

$$\tilde{v}_P = v_p^* + (p_{i,j-1} - p_{i,j}) \frac{\Delta t}{\rho \delta y_j} \tag{2-36}$$

The values of u_p* and v_p* represent initial "guess" values based upon previous time step velocity values and current source term influences, but omitting pressure, as shown below.

$$u_P^* = \left[b^u + a_P^u u_P + a_N^u u_N + a_E^u u_E + a_S^u u_S + a_W^u u_W \right] \frac{\Delta t}{\rho \Delta V^u} \tag{2-37}$$

$$v_P^* = \left[b^v + a_P^v v_P + a_N^v v_N + a_E^v v_E + a_S^v v_S + a_W^v v_W \right] \frac{\Delta t}{\rho \Delta V^v} \tag{2-38}$$

The integral form of the mass conservation equation is integrated over the main grid CV (as illustrated in Figure 2-2). Performing this integration at time step $n+1$, yields:

$$(u_{i+1,j}^{n+1} - u_{i,j}^{n+1}) \Delta y_j + (v_{i,j+1}^{n+1} - v_{i,j}^{n+1}) \Delta x_i = 0 \tag{2-39}$$

Substituting equations (2-33) and (2-34) into equation (2-39), and re-writing the resulting expression in terms of the pressure correction $\delta p_{i,j}$ at node i,j gives the following:

$$a_P^p \delta p_{i,j} = a_N^p \delta p_{i,j+1} + a_E^p \delta p_{i+1,j} + a_S^p \delta p_{i,j-1} + a_W^p \delta p_{i-1,j} + b^p \tag{2-40}$$

where the coefficients are defined as follows:

$$a_N^p = \frac{\Delta x_i \Delta t}{\rho \delta y_{j+1}} \quad ; \quad a_E^p = \frac{\Delta y_j \Delta t}{\rho \delta x_{i+1}} \tag{2-41a,b}$$

$$a_S^p = \frac{\Delta x_i \Delta t}{\rho \delta y_j} \quad ; \quad a_W^p = \frac{\Delta y_j \Delta t}{\rho \delta x_i} \tag{2-41c,d}$$

$$a_P^p = a_N^p + a_E^p + a_S^p + a_W^p \tag{2-41e}$$

$$b^p = (\tilde{u}_{i,j} - \tilde{u}_{i+1,j})\Delta y_j + (\tilde{v}_{i,j} - \tilde{v}_{i,j+1})\Delta x_i \tag{2-41f}$$

The pressure correction equation (2-40) is solved for all full cells in the domain. If a given full cell has all four neighbours that are also full, the coefficients of the equation are determined by the use of equations (2-41). If one or more of its neighbours is a surface cell, however, the coefficient corresponding to each of these neighbours must be modified. This process enables the enforcement of the surface boundary condition, and is described in the following section.

2.6 Boundary Conditions

To complete the specification of the discretized equations it is necessary to account for the behaviour of the fluid at the boundary of its domain. One must include in the method a means of incorporating boundary conditions that is both physically realistic and as simple as possible to implement. The following sub-sections discuss how this is accomplished for the free surface and for rigid boundaries. For rigid boundaries the procedure is elementary, but for the free surface boundary, the procedure must take into account the fact that the surface configuration changes from one time step to the next.

2.6.1 Free Surface Boundary

In the modelling of fluid problems with a free surface interface, there are four requirements which must be met. These are:

1. Allowing the free surface to move freely in a manner that is physically realistic;
2. Tracking the free surface continuously as it moves;
3. Defining the surface with a spatial resolution that is sufficient for the design problem at hand; and
4. Imposing the boundary conditions applicable to the free surface.

The chosen approach is the Volume of Fluid (VOF) method, as described by Hirt and Nichols [13], and exemplified by the SOLA-VOF computer program [14]. As discussed in Chapter1, the VOF method offers several advantages over alternative methods such as marker particles and height functions. As will be evident in the following discussion, the VOF method satisfies the needs stated above.

The VOF method is based upon the evaluation of a variable called F for each (main grid) control volume. This value F gives the fraction of the total volume of the cell that is occupied by fluid. In other words, an empty cell has an F value equal to zero, a full cell has F equal to unity, and a partly-full cell has a value somewhere between these two limits. A partly-full cell by definition contains a free surface. The calculation domain for momentum and continuity at any point in time is defined by the sum of all those cells that are not empty. The set of partly-full cells together form the free surface boundary, or boundaries, for the domain.

Within the domain, the time dependence of F is governed by the following equation.

$$\frac{\partial F}{\partial t} + u\frac{\partial F}{\partial x} + v\frac{\partial F}{\partial y} = 0 \qquad (2\text{-}42)$$

To allow the free surface to move through the Eulerian grid, an algorithm to convect flux from one cell to another is required. By first integrating equation (2-42) over the main grid CV, one can obtain a donor-acceptor method. The method is described more thoroughly in [13], and will only be stated here.

The amount of F fluxed in the x-direction across a cell face in one time step is δF^u multiplied by the face cross-sectional area (i.e. Δy_j), where

$$\delta F^u = \text{MIN}\left\{F_{AD}|Q^u| + CF^u \ , \ F_D \Delta x_D\right\} \qquad (2\text{-}43)$$

and

$$CF^u = \text{MAX}\left\{(F_{DM} - F_{AD})|Q^u| - (F_{DM} - F_D)\Delta x_D \ , \ 0.0\right\} . \qquad (2\text{-}44)$$

In these equations, the maximum possible flux volume per unit area across a cell face is Q^u, where $Q^u = u_{i,j}\Delta t$. The subcript A indicates the "acceptor" cell, D refers to the "donor" cell, and subscript AD means that either A or D is selected, depending on the orientation of the free surface in relation to the direction of flow. The subscript DM indicates the F value of the cell upstream of the donor cell, and the use of this term tends to dampen the flux when the upstream cell is not full. This term is only found in the SOLA-VOF code; textual references in all articles use the value 1.0 in its place. This author experimented with both approaches and found that the use of F_{DM} causes no apparent weakness in the algorithm. The

determination of which cell is the donor and which is the acceptor is a function only of the direction of the flow. The MIN function prevents convecting more fluid from the donor cell than it has to give, and the MAX function ensures that a donor cell fluxes only that amount that exceeds the volume needed to fill it.

Equations corresponding to (2-43) and (2-44) are obtained for the y-direction velocities as well. A complete update of F values for the advanced time level consists of a pass over the whole domain adding and/or subtracting changes in F value to the current F values, first for the x-direction fluxes, and then in the y-direction.

To accomplish the tracking of the free surface, the surface is defined as passing through the cells which have an F value between zero and one, and which have at least one empty neighbouring cell.

The method of specifying a boundary condition at the free surface is to specify the pressure on the surface. For a vented tank with air as the fluid above the denser liquid, this value is atmospheric pressure. Since pressure values are located at the cell centers, this is accomplished by assigning surface cells a pressure that is an interpolation between the free surface and the value at a selected neighbour cell, as shown in Figure 2-4. The formula is:

$$p_{FS} = p_{int}(1 - \eta) + \eta p_{surf} \tag{2-45}$$

where

$$\eta = \frac{d_c}{d} \tag{2-46}$$

and p_{FS} is the pressure of the free surface cell, p_{int} is the pressure at the interpolation cell center, and p_{surf} is the specified surface pressure. The variable η is the ratio of distances as defined is Figure 2-4. For example, with a surface cell at node $i+1, j$, and its interpolation neighbour at cell i, j , equations (2-45) and (2-46) become:

$$p_{i+1,j} = p_{i,j}(1 - \eta_{i+1,j}) + \eta_{i+1,j} p_{surf} \quad , \tag{2-47}$$

where

$$\eta_{i+1,j} = \frac{\delta x_{i+1}}{0.5\Delta x_i + F_{i+1,j}\Delta x_{i+1}} \quad . \tag{2-48}$$

For a given free surface cell, it is necessary to determine which of its neighbouring cells will act as the interpolation neighbour. The neighbour for which a line connecting the two cell centers forms an angle with the free surface that is closest to a right angle, is the cell designated as the interpolation neighbour. To make this judgement, an estimation of the orientation of the free surface in a given free surface cell must be made. This is done by representing a local segment of the free surface in a cell centered at i,j by a single-valued function $\psi(x)$, indicating the y-distance of the surface above a datum. The function is calculated [14] as:

$$\psi_i = \psi(x_i) = F_{i,j-1}\Delta y_{j-1} + F_{i,j}\Delta y_j + F_{i,j+1}\Delta y_{j+1} \tag{2-49}$$

and the change of ψ with increasing x can be most simply approximated by

$$\left(\frac{d\psi}{dx}\right)_i = \frac{(\psi_{i+1} - \psi_{i-1})}{(\delta x_i + \delta x_{i+1})} \quad . \tag{2-50}$$

Similarly, the distance of the free surface in the x - direction measured from a datum can be denoted $\chi(y)$; the local value and its derivative with respect to y are calculated as follows.

$$\chi_j = \chi(y_j) = F_{i-1,j}\Delta x_{i-1} + F_{i,j}\Delta x_i + F_{i,j+1}\Delta x_{i+1} \tag{2-51}$$

$$\left(\frac{d\chi}{dy}\right)_j = \frac{(\chi_{j+1} - \chi_{j-1})}{(\delta y_j + \delta y_{j+1})} \tag{2-52}$$

If the magnitude of $(d\chi/dy)$ is the lower of the two slopes, the surface is more nearly vertical than horizontal, and the sign of $(d\psi/dx)$ indicates whether the fluid cell is on the right or left of cell i, j. Conversely, if the magnitude of $(d\psi/dx)$ is the lower, the surface is more nearly horizontal, and the sign of $(d\chi/dy)$ will define if the fluid is above or below cell i, j. The slope information can also be useful in constructing the surface for visual presentation.

To impose the boundary condition of specified pressure on the free surface, it is necessary to modify one or more coefficients of the pressure equation for all cells which are full and have one or more neighbours which are surface cells. For the case of full cell i,j with surface configuration given in Figure 2-4, this is done by first re-writing (2-47) in terms of the advanced time level pressures, using (2-32):

$$p^{n+1}_{i+1,j} = p^{n+1}_{i,j}\,(1 - \eta_{i+1,j}) + \eta_{i+1,j}P_{surf} \tag{2-53}$$

and

$$\delta p_{i+1,j} = (p_{i,j} + \delta p_{i,j})\,(1 - \eta_{i+1,j}) + \eta_{i+1,j}P_{surf} - p_{i+1,j} \tag{2-54}$$

The substitution of this expression into equation (2-40) results in the modified coefficients as

follows:

$$a_E^P = 0 \tag{2-55a}$$

$$a_P^P = a_N^P + a_W^P + a_S^P + \left(\frac{\Delta y_j \Delta t}{\rho \delta x_{i+1}} \right) \eta_{i+1,j} \tag{2-55b}$$

$$b^P = (\tilde{u}_{i,j} - \tilde{u}_{i+1,j}) \Delta y_j + (\tilde{v}_{i,j} - \tilde{v}_{i,j+1}) \Delta x_i + \frac{\Delta y_j \Delta t}{\rho \delta x_{i+1}} \left[(1 - \eta_{i+1,j}) p_{i,j} + \eta_{i+1,j} p_{surf} - p_{i+1,j} \right] \tag{2-55c}$$

The coefficients a^P_W remain unchanged, unless cell i,j is also the interpolation neighbour for either of its west neighbours as well. In that case, the relevant coefficients are modified in a similar manner. If cell i,j acts as the interpolation neighbour for its north or south neighbours as well, the appropriate coefficients are also modified.

2.6.2 Rigid Boundaries

The tank walls constitute the rigid boundaries for the fluid domain, and for the method described in this thesis, are straight and aligned with the grid. Pressure nodes do not coincide with the walls, but u and v velocities are located on these boundaries, therefore, it is straightforward to enforce velocity boundary conditions there. Velocities perpendicular to a given wall are set equal to zero. Velocities parallel to a wall are assigned to enforce free slip conditions: the boundary values for an advanced time step are set equal to those closest internal (calculated) values from the previous time step. For example, u values on the south boundary (tank bottom) are set equal to those at the next j index to the north resulting from the previous time step. No-slip conditions were not imposed in the tests presented in this

thesis, because it was necessary to concentrate on the free surface dynamics. Accurate definition of the boundary layer would require a refined mesh and increased processing time.

These boundary velocity values are incorporated into the momentum calculations through equations (2-37) and (2-38), and into continuity by equation (2-41). For cells which serve the purpose of enforcing the free surface boundary condition, and also border on a tank wall, equation (2-55c), and/or similar equations for the b coefficient, use the boundary velocity values directly.

2.7 Solution Algorithm

The calculation process begins with a pressure-velocity field that is known throughout the domain. The domain is that part of the Eulerian calculation grid which is fluid-occupied at the current time step. The domain is then updated by convecting F between neighbouring cells, resulting in a new free surface configuration, which applies to the advanced time level. It is then necessary to determine the pressure-velocity field for the new domain.

The process used is to solve in sequence for velocity, pressure correction, and pressure, repeating the procedure until the field has converged to satisfactory level. The first step in this process is to calculate the initial guess or starred velocities explicitly from the values for the previous time step using equations (2-37) and (2-38). Initial values of tilde velocities (equations (2-35) and (2-36)) are then determined, and subsequently used to calculate coefficients for the pressure correction equation, equations (2-41), along with all contributions from solid and free surface boundaries where applicable.

The series of equations represented by equation (2-40) can be solved by various techniques to obtain a set of pressure corrections. A point-by-point relaxation method has been chosen for its simplicity, but line-by-line or block relaxation methods are not appropriate, because they would be tedious to apply to a domain which changes and may result in rows or columns of related cells being discontinuous. Hence, the pressure corrections are found by application of the following equations over all (main grid) control volumes that are full of fluid.

$$\Sigma^p = a_N^p \delta p_{I,J+1} + a_E^p \delta p_{I+1,J} + a_S^p \delta p_{I,J-1} + a_W^p \delta p_{I-1,J} \tag{2-56}$$

$$\delta p_{I,J} = \frac{\Sigma^p + b_{I,J}^p}{a_P^p} \tag{2-57}$$

Repeated applications of the solver are needed, until the pressure corrections converge, and the continuity equation is simultaneously satisfied to an acceptable level of accuracy. The acceptable accuracy is achieved when the residual of the pressure correction equation (2-40) is sufficiently small, or, in other words, less than a specified tolerance denoted ∇_{test}, for all CVs. This is stated by:

$$\left| a_P^p \delta p_{I,J} - \Sigma^p - b_P^p \right| < \nabla_{test} \tag{2-58}$$

To enable a complete and accurate calculation process to be carried out, it is necessary for the following factors to be taken into account. First, the momentum equations are solved for every velocity control volume for which both main grid CVs contain fluid. When the corrections of velocity are made for a (staggered grid) CV that is not 100 % full, a modification of the pressure force term is neccesary to account for the reduced mass. This

is accomplished by using a modified δx_i (or δy_j), reducing it in proportion to the F values of component main grid cells. This is done for instances where the free surface in either or both of the main grid cells is oriented in the same general direction as the velocity being considered. Therefore, in all equations in which the pressure gradient occurs (e.g. equations (2-35) and (2-36)), δx is replaced by an effective value δx_{eff}. Similarly, δy is replaced by δy_{eff}, defined as follows:

$$\left(\delta x_{eff}\right)_i = 0.5\left[F_{i-1,j}\Delta x_{i-1} + F_{i,j}\Delta x_i\right] \tag{2-59}$$

$$\left(\delta y_{eff}\right)_j = 0.5\left[F_{i,j-1}\Delta y_{j-1} + F_{i,j}\Delta y_j\right] . \tag{2-60}$$

The second consideration is that in order to perform the calculation of the starred velocity values, and to permit flux from a surface cell to a previously empty cell during an update of the F values, it is necessary to calculate velocity values at points just outside the free surface. These are essentially velocity boundary conditions set in the vicinity of the free surface. The values are calculated by enforcing continuity on the free surface control volumes. In addition, since the F-convection calculations use flux transfer areas based upon donor/acceptor cell F-values, the calculation of free surface velocity boundary values must take these F-values into account, to ensure that continuity is preserved as accurately as possible when performing VOF updates.

The final factor is the need for a tolerance for use in testing whether a main grid CV is full, empty, or partly filled. It is considered that a cell is empty if its F value is less than a small number, denoted ϵ; a value of 10^{-5} was used with success in this research. Similarly, a cell

is considered to be full if its F value is greater than $(1 - \epsilon)$. A cell is a surface cell if its F value is between these two inclusive limits. To preserve this system of surface identification, and prevent dispersion of the surface, a housekeeping check is done after each VOF update, revising all nominally full cell F values to unity, and F for all nominally empty cells to zero. Also, any cell which is full at that point, but which has at least one empty neighbour, is reverted to a surface cell by re-setting its F value to $(1 - 1.1\epsilon)$. The change in total fluid volume is accumulated and can be inspected at any time; the change is always less than 0.1 percent of the initial total volume after a run of tens of thousands of time steps.

2.8 Summary

The method used in this research, to model the sloshing of fluid in a partly filled tank, is summarized by the following sequence of operations:

1. Initial values of all necessary data are assigned. These include number of calculation cells, grid spacings, time interval limits, tank fill fraction, tank dimensions, fluid properties, surface pressure, initial values for fluid velocities, initial values and constants for tank motion, subroutine flags, iteration counters, and other calculation parameters. Initial values of fluid pressure and F are calculated based on these data.
2. Velocity boundary conditions are updated, both for the tank walls and the free surface.
3. The time interval for the next step is determined.
4. Tank motion parameters for the advanced time step are calculated, according to the prescribed tank motion.
5. The set of F values is updated, by convecting the fluid between neighbouring cells with the current velocity and surface configuration. The result is a revised

surface configuration.

6. The interpolation cells for all surface cells are identified. All cells are assigned a code which indicates their status in terms of being full, empty, or surface, and, when applicable, for which neighbour(s) they act as interpolation cell.

7. Initial guesses for new velocities u^* and v^* are calculated using equations (2-37) and (2-38).

8. Initial values for the coefficients of the pressure correction equation, equation (2-40), are calculated.

9. The values of pressure and velocities are corrected with pressure corrections to yield a converged solution to the flow field. The process is as follows:

(a.) Pressure corrections are solved, for all full cells, using several sweeps of the domain by a point-by-point relaxation scheme, equations (2-56) and (2-57);

(b.) Pressure and velocity are corrected using corresponding pressure corrections. Pressures for all full cells are first corrected using equation (2-32); relaxation of the pressure change may be employed at this stage, if desired. Secondly, the pressures for surface cells are calculated using the interpolation formula, e.g. equation (2-47). Surface cells with interpolation neighbours that are full are dealt with, and then surface cells with interpolation neighbours that are partly full are addressed. Thirdly, the new velocity values are obtained by correction with pressure for all cells, using equations (2-35) and (2-36);

(c.) the residual of the pressure correction equation is calculated for all full cells, and if any of these values is greater than the specified tolerance, and the

maximum allowable number of iterations per time step has not been reached, one returns to step 9(a). Otherwise one continues to step 10.

10. The resulting converged flow field can then be written to file, for use in presentation and analysis. If neither the time step counter or run time has exceeded their specified maximums, the "old" velocities are assigned the values of the new configuration, and one returns to step 2.

The obtained flow fields, along with F values for definition of the free surface configuration, are printed at selected time intervals and the collected set of data are stored in sequential series, allowing visual presentation of the sloshing behaviour. Sample problems simulated using this method are described in the following chapter.

Chapter 3

Results

The method described in the previous chapter was implememted in a FORTRAN program. The program and method were tested in the context of several sample problems using the DEC 4000/610 computer system at the Centre for Computer-Aided Engineering of Memorial University of Newfoundland. The FVM used to discretize the governing equations was initially tested separate from the the free surface algorithm using standard test cases. The method was successful in these cases. The results of these tests are not reported here, because the main interest in this thesis is sloshing, i.e. free surface behaviour.

The sample problems presented in this chapter are: (1) rotation to a specified angle; (2) translation at a natural frequency; (3) impulsive translation ; (4) translation near the natural frequency; (5) continuous rotational motion, and (6) combined translation and rotation. The following sections discuss these test cases and the resulting fluid field data generated by the proposed method. A summary of the results obtained is presented in the final section of this chapter.

3.1 Rotation of theTank to a Specified Angle

To validate the VOF algorithm, the method was used to simulate the rotation of the tank about its lower left corner, i.e. the origin of the (x,y) frame. The motion of the tank was

described by the following equations:

$$\theta_2 = \theta_{2\,max} \cos\left(\frac{2\pi t}{T_\theta}\right) - \beta_2 \tag{3-1}$$

$$\omega_2 = -\theta_{2\,max} \frac{2\pi}{T_\theta} \sin\left(\frac{2\pi t}{T_\theta}\right) \tag{3-2}$$

$$\alpha_2 = -\theta_{2\,max} \left[\frac{2\pi}{T_\theta}\right]^2 \cos\left(\frac{2\pi t}{T_\theta}\right) \tag{3-3}$$

The specified tank motion was as follows: the initial value of the tank inclination angle, β_2, was set at 2.0 degrees, and the value of $\theta_{2\,max}$ was 2.0 degrees. The angular displacement, velocity, and acceleration of the tank about the (x,y) axis were calculated using equations (3-1), (3-2), and (3-3), respectively, for a duration of one specified period of rotation, T_θ. After that time θ_2, ω_2, and α_2 are held constant at zero. This sequence generates an initial motion in the fluid domain, which is expected to decay. The ideal fluid configuration, as indicated by the set of F values, is a straight line tilted at an angle of β_2, but in the opposite sense. The test was performed on an equally-spaced grid, with 20 × 20 main grid nodes.

The test run was performed on a tank with height of 1.0 meter, length of 1.0 meter, and a fill fraction of 0.725 of the tank height. A density of 1000 kg/m^3 was used, and viscosity was 10.0 kg/m·s. This viscosity value corresponds to a relatively viscous liquid, and will encourage dampening of wave motion. The time step used was 1×10^{-4} s for the first 10.0 seconds, and 5×10^{-4} s thereafter.

The resulting heights of the fluid surface at the left and right walls of the tank are plotted

against time in Figure 3-1. As can be seen in this figure, the fluid surface experienced the expected behaviour of overshooting the final static position, and then oscillating about these height values, with the oscillations eventually decaying. The final mean elevations on the left and right walls are 0.7405 m and 0.7125 m respectively. The expected elevations are 0.7416 m and 0.7084 m, giving percentage errors of -0.15 % and 5.7 % on the left and right walls, respectively. The period of the oscillations of the fluid heights is measured as 1.3 seconds (the data was output at 0.2 second intervals), which compares favourably with the expected natural period of 1.133 s. The shape of the free surface at the end of the calculation is shown in Figure 3-2. As shown in this figure, there is a mild bow in the surface, but a check of the fluid volume shows that only 6.1×10^{-7} % of the volume was gained at the end of the calculation, in which 319610 time steps elapsed.

3.2 Tank Translation at Natural Period

The sloshing behaviour of a fluid is defined in part by the period of oscillation at which standing waves propogate within the tank. Several modes of standing water wave vibration are possible [31], but the mode with the longest period is the one most likely to be excited by ocean wave motion [32]. This natural period is approximated, using linear wave theory for water of a finite depth [5,32], by the following relationship:

$$T_N^2 = \frac{4\pi L}{g \tanh\left(\frac{\pi h}{L}\right)} \tag{3-4}$$

where L is the length of the tank (x - direction), h is the average height of fluid in the tank, g is the acceleration due to gravity, and T_N is the period of the resonant oscillation. The wavelength of this mode of vibration is twice the length of the tank.

To verify the physical accuracy of the numerical method, it is necessary to confirm that the algorithm produces fluid motion which agrees well with the theoretical natural resonance. When the specified tank motion is oscillatory and has a period equal to that of a theoretical natural mode of vibration, the predicted behaviour is that wave amplitude would increase without limit. In addition, it is expected that the motion of the fluid surface at the left wall of the tank would be 180 degrees out of phase with that at the right wall.

The following test was devised to evaluate the fluid motion in a tank undergoing oscillatory excitation at a natural frequency. A square tank with dimension L = 1.0 meter was given an average fill height h = 0.725 meters. The specified tank motion consisted of a pure translation in the x-direction, defined by the following expressions:

$$r_1 = r_{1\,max} \cos\left(\frac{2\pi t}{T_r}\right) \tag{3-5}$$

$$\dot{r}_1 = -\, r_{1\,max} \left[\frac{2\pi}{T_r}\right] \sin\left(\frac{2\pi t}{T_r}\right) \tag{3-6}$$

$$\ddot{r}_1 = -\, r_{1\,max} \left[\frac{2\pi}{T_r}\right]^2 \cos\left(\frac{2\pi t}{T_r}\right) \tag{3-7}$$

where $r_{1\,max}$ is the amplitude of the displacement, and the period of the translatory motion is T_r. The value of $r_{1\,max}$ was 2 millimeters, while T_r was set as 1.13 seconds. For this test, the first mode of vibration was simulated; the predicted natural period of surface wave motion is 1.133 seconds, as determined by equation (3-4). All angular motion inputs were set equal to zero. The fluid properties used in this problem were ρ = 1000 kg/m^3 and a viscosity

of 10.0 kg/m·s, while the time step was 5×10^{-5} s for the first 5 seconds and 1×10^{-4} s from then onward. The test was performed on a equally-spaced grid, with 20 × 20 main grid nodes.

As shown in Figure 3-3, the fluid heights at the left and right walls of the tank increase continually due to excitation of the tank at the natural frequency. The amplitude of the motion is larger than 2.5 cm after four periods of excitation, whereas the input amplitude was only 2 millimeters. The period of the sloshing is 1.092 s, which compares favourably with the predicted value of 1.133 s. The fact that the motions at the two opposite walls are out of phase is apparent by inspection.

3.3 Impulsive Translation of the Tank

The response of the free surface to an initially impulsive tank motion would give an indication of the sensitivity of the method to sudden changes in input motion, and provide an additional verification of the ability of the method to capture the natural frequency of the free surface motion. To specify an impulsive horizontal tank motion, equations (3-5), (3-6), and (3-7) were used to determine the displacement, velocity and acceleration of the tank. This motion was employed only for one half of a period, after which the position of the tank was fixed.

In this problem the value of $r_{I\,max}$ was specified to be 2 centimeters, and the value of T_r was 2.0 seconds. The tank height was set at 1.0 meter, tank length L = 1.0 meter, and the average fill height h = 0.425 meters. Density was 1000 kg/m^3, viscosity was 10.0 kg/m·s, and the test was performed on a equally-spaced grid, with 20 × 20 main grid nodes. The time step was 1×10^{-3} s for the first 20 seconds, 2×10^{-3} s thereafter.

The resulting surface motion is shown by the plot of the height of the fluid at the right wall of the tank, as shown in Figure 3-4. The oscillatory motion of the fluid decays and the period is 1.16 seconds, which compares well with a second mode natural period of 1.20 seconds, calculated from linear theory. A plot of numerical results (using a MAC-based method) and experimental data is found in Popov et al. [21]. The input impulse translation function used by Popov could not be reproduced for this test; however, the results in [21] show a form of wave behaviour similar to Figure 3-4, and the period of natural resonance is also observed to be close to that predicted. It is not valid to compare wave heights between these two results.

3.4 Tank Translation Near the Natural Period

If a linear system is forced to oscillate at a frequency that is close to its natural frequency, the resulting system response consists of alternating periods of amplitude re-inforcement and cancellation. The resulting waveform exhibits what is known as beating. The period of the beating waveform can be predicted from the following simple equation:

$$T_B = \frac{2}{\left| \frac{1}{T_F} - \frac{1}{T_N} \right|} \tag{3-8}$$

where T_B is the period of the combined waveform, and T_F is the period of the forcing motion, and T_N is the natural period of the system.

The translatory motion was specified using equations (3-5), (3-6), and (3-7). In this problem, the value of $r_{1\,max}$ was specified to be 5 millimeters, and the value of T_r was 1.5 seconds. The tank was square with L = 1.0 meter, and the average fill height h was set at 0.725 meters.

Density was 1000 kg/m^3, and viscosity was 1.0 kg/m·s. The time step used was 1×10^{-3} s for an initial 5.0 seconds, and 2×10^{-3} s afterward. The natural period of the first mode of vibration for this system is 1.133 s (as found using equation (3-4)), and using equation (3-8) a beating period of 9.26 seconds is predicted. An equally-spaced grid was employed, with 20 × 20 main grid nodes.

The resulting behaviour of surface heights at the left and right walls are plotted as functions of time in Figure 3-5. The beating phenomenon is clearly seen in the waveform. The resulting period of beating is 7.94 seconds, which is within 14.5 % of the predicted value. This error is attributed to the use of linear theory for the beat period, in a problem where non-linearities are present in the physical system. These non-linearities are accounted for in the proposed method.

3.5 Tank Rotation

Tests were also performed to confirm the effective operation of the numerical model with the forced tank motion specified as one of rotation only. The angular motion of the tank about its bottom left corner is specified through the use of equations (3-1), (3-2), and (3-3).

A test was done with β_2 equal to 3.0 degrees, $\theta_{2\,max}$ equal to 3.0 degrees, and T_0 set at 10.0 seconds. This motion is intended to be representative of rolling motion which may experienced on the deck of a ship at sea. The tank dimensions were 1.0 by 1.0 meters, the average fill height was 0.725 m, density was set at 1000 kg/m^3, and dynamic viscosity was 10.0 kg/m·s. The time steps used were 5×10^{-4} s for the initial 25 seconds, and 1×10^{-3} s afterwards. The test was performed on an equally-spaced grid, with 20 × 20 main grid nodes.

The results for this test are illustrated by Figure 3-6, which presents the fluid heights at the left and right walls of the tank. In Figure 3-6, one can see that the natural period waves continue to exist when the tank is forced to oscillate with a much higher period, even with relatively high viscosity, resulting in the superposition of the two waves.

3.6 Tank Rotation and Translation

The ability of the numerical model to determine the motion of the liquid under a more complex tank motion was tested. The simultaneous rotation and translation of the tank is of interest because the configuration is a reasonable two-dimensional representation of the real motion of a ship at sea. The test problem presented here is representative of simultaneous roll and sway.

For this problem, the angle θ_2 and its rates of change, were specified in accordance with equations (3-1), (3-2), and (3-3), and the displacement r_1, along with the corresponding velocity and acceleration, were specified using equations (3-5), (3-6), and (3-7). The period of oscillation was 10.0 seconds for the angular motion, and 8.0 seconds for the translation. Rotation angle amplitude was set at 2.0 degrees, and $r_{1\,max}$ was 5 centimeters, while β_2 was 2.0 degrees. The tank size was square with length of 1.0 m; a density of 1000 kg/m^3 was used, and a dynamic viscosity of 15.0 kg/m·s was specified. The time step was 1×10^{-3} s for the first 50 seconds, and 2×10^{-3} s thereafter. The test was performed on a equally-spaced grid, with 20 × 20 main grid nodes.

The results of this test are illustrated by Figures 3-7, 3-8, 3-9, and 3-10. Figure 3-7 is a plot

of the fluid heights at the left and right walls. While there is a wave period of about 10 seconds evident from the graph, there is a peak in amplitude occuring about every 40 seconds. Figure 3-8 shows eleven sequential images of the free surface. The first image occured at t = 60.0 s, the last image occured at 65.0 s, and the intervening plots occur at various intervals. It should be noted that the range and scale on the vertical axis are different from that of the horizontal axis. This figure gives an indication of the shape of the surface, and how it changed over a period of time. Figure 3-9 is a vector plot of the velocity field at time t = 62.5 seconds. As shown in this figure, the fluid has a clockwise circulation, with a maximum velocity of 0.0683 m/s, which occurs on the surface. Figure 3-10 is similar velocity vector plot for t = 67.5 s. In this plot it can be seen that the circulation is counter-clockwise, the maximum velocity is 0.0602 m/s, and it also occurs on the surface. These figures are "snapshots" of the fluid motion when the fluid height is approximately uniform across the length of the tank (i.e. at the average fill height, h). In Figure 3-9 the fluid height at the left wall is beginning to decrease and the tank angle of rotation θ_2 is negative and decreasing at its maximum rate. In Figure 3-10 the fluid height at the left wall is beginning to increase and the tank angle of rotation θ_2 is negative and increasing at its maximum rate. These figures indicate a calculated fluid behaviour which is qualitatively consistent with expected behaviour.

3.7 Summary

The results presented in this section demonstrate that the proposed method can model the two-dimensional sloshing in a rectangular tank in a manner which is consistent with expected physical behaviour. The ability of the method to reliably track the free surface was confirmed by a test in which the inclination angle is first disturbed and subsequently held constant. The capability of producing resonant wave motion was tested successfully by using a tank

excitation at the predicted natural period for the tank. This existence of this natural period was also supported by all of the other tests which were done, where higher frequency oscillations could be seen. A test in which an impulsive tank translation is specified served to validate the natural period of oscillation, and to demonstrate the existence of dampening due to viscosity. The test using a tank motion with a period near the theoretical natural period produced the expected wave behaviour, exhibiting alternating cancellation and reinforcement, and the beating period was of the same order as that predicted for a linear system. Tests conducted with tank motion representing sustained rotational oscillations only (i.e. vessel roll), and a combined rotation and translation (i.e. roll and sway) demonstrated the capability of the method to simulate realistic container motions.

Chapter 4

Conclusions

4.1 A Review of the Thesis and its Contributions

This thesis presents the development and implementation of a Finite Volume Method (FVM) to simulate the sloshing behaviour of incompressible, constant density liquids in a two-dimensional, rigid rectangular tank. The FVM is used to discretize the governing momentum and mass conservation equations using primitive variables in a fully Eulerian approach. The method is formulated by integrating the governing equations over appropriate control volumes, and assembling systems of linear equations. A fixed rectangular grid with variable spacing is utilized, and momentum control volumes (CVs) are staggered with respect to continuity CVs. The inertial accelerations caused by a specified tank motion are applied to the fluid by the inclusion of additional source terms in the momentum equations. The FVM incorporates upwinding directly, allows the direct specification of velocity boundary conditions on the tank walls, and offers an advantage in simplicity over Eulerian and Lagrangian finite element methods. The flow regime is advanced through time using a pressure correction solution process.

The free surface boundary is handled using the Volume of Fluid (VOF) method, which tracks the movement of the region(s) occupied by fluid, as opposed to tracking the movement of the free surface interface. The VOF method is based on the assignment of a variable F for each

continuity control volume, where F represent the average fraction of the cell volume which is occupied by fluid. The approach permits arbitrary movement of the surface, including the possibility of overlapping and smaller regions breaking away.

This research work has two unique aspects. The first is the application of both an FVM and the Volume of Fluid method to this particular free surface problem: sloshing in a tank. The second, and more significant characteristic of the proposed method is the ability to accommodate the simultaneous translation and rotation of the tank relative to the absolute reference frame, and rotation of the tank about its local reference frame. This ability allows a general tank motion to be defined, enabling the analysis of realistic design problems. In other similar published research, the tank motion has been limited to either translation or rotation.

Various tests have been carried out on the proposed method, with tank motions prescribed to verify: (i) the ability of the method to produce the wave motion with frequency characteristics predicted by theory; and (ii) the ability of the method to perform with combined translation and rotation. The results of these tests have been presented, and are successful in meeting these two requirements.

4.2 Proposed Extensions of This Work

There are two principle directions in which further research should continue. These are: (i) continued verification and optimization of the proposed two-dimensional numerical model; and (ii) the extension of the proposed method to three dimensions.

The proposed method has been shown to produce fluid wave motions that exhibit frequency characteristics which are realistic and conform to theory. The following additional testing of this two-dimensional model is necessary:

(1) Further work is required to verify that the surface heights produced conform to theoretical predictions and physical experiments.

(2) Optimization of the calculation parameters is recommended. The most effective combinations of the following parameters must be sought, to allow the mapping of the full extent of the capabilities of the method. The parameters are:
   (a) time step;
   (b) grid size;
   (c) non-uniform grid spacings;
   (d) number of iterations of the point-by-point relaxation solver (in the calculation of pressure corrections);
   (e) relaxation factors for pressure and velocity;
   (f) tank aspect ratios and fill fractions, particularly to identify hydraulic jump behaviour; and
   (g) other values of density and dynamic viscosity which may be of interest.

The proposed method has been shown to be capable of determining the fluid behaviour in a tank undergoing rotation about its local frame, and translation relative to the fixed frame. Additional testing of the method is needed for tank motions which are fully general (i.e. a ship motion combination of roll, sway, and heave), and for more extreme motions. The more

extreme motion would include, for example, large angular displacements, complete overturning of the tank, and impact of waves on the tank ceiling. A desirable motion scenario to implement would be one which results in a second region of fluid breaking away from the main body of fluid.

It is also recommended that a version of this method be developed for a three-dimensional rectangular tank. Such a version would be necessary to ensure broad application to many design problems involving the transport of liquids, including roll stabilization tanks consisting of connected rectangular compartments.

References

1. Hamlin, N.A., Lou, Y.K., Maclean, W.M., Seibold, F., and Chandras, L.M., "Liquid Sloshing in Slack Ship Tanks - Theory, Observations, and Experiments", *SNAME Transactions*, Vol. 94, pp. 159-195, 1986

2. Bass, R.L., Bowles, E.B., and Cox, P.A., "Liquid Dynamic Loads in LNG Cargo Tanks", *SNAME Transactions*, Vol. 88, pp. 103-126,1980

3. Tanaka, T., Endo, S., Isozaki, S., Kobayashi, T., Imamura, T., and Saito,M., "Estimation of Impact Pressure and Hydrodynamic Force Due to Sloshing in LNG Carrier", *Nipon Kokan Technical Report, Overseas*, No. 84, pp. 80-93,1984.

4. Van den Bosch, J.J., and Vugts, J.H., "On Roll Damping by Free Surface Tanks", *Royal Institution of Naval Architects Transactions*, Vol. 108, pp. 345-361, 1966.

5. Faltinsen, O.M., *Sea Loads on Ships and Offshore Structures*, Cambridge University Press, New York, 1990.

6. Faltinsen, O.M., "A Nonlinear Theory of Sloshing in Rectangular Tanks", *Journal of Ship Research*, Vol. 18, No. 4, pp. 224-241,Dec. 1974.

7. Harlow, F.H., and Welch J.E., "Numerical Calculation of Time-Dependent Viscous Incompressible Flow of Fluid with Free Surface", *The Physics of Fluids*, Vol. 8, No. 12, pp. 2182-2189, Dec. 1965.

8. Viecelli, J.A., "A Method for Including Arbitrary External Boundaries in the MAC Incompressible Fluid Computing Technique", *Journal of Computational Physics*, Vol. 4, pp. 543-551, 1969.

9. Nichols, B.D., and Hirt, C.W., "Improved Free Surface Boundary Conditions for Numerical Incompressible Flow Calculations", *Journal of Computational Physics*, Vol. 8, pp 434-448, 1971.

10. Amsden, A.A., and Harlow, F.H., "The SMAC Method: A Numerical Technique for Calculating Incompressible Fluid Flows", *Los Alamos Scientific Laboratory of the University of California, Report LA-4370*, 85 pages, 1970.

11. Chan, R.K.-C., and Street, R.L., "SUMMAC -- A Numerical Model for Water Waves", *Department of Civil Engineering, Technical Report No.135*, Stanford University, 165 pages, 1970.

12. Hirt, C.W., Nichols, B.D., and Romero, N.C., "SOLA - A Numerical Solution Algorithm for Transient Fluid Flows", *Los Alamos Scientific Laboratory Report LA-5852*, 51 pages, April 1975, Addendum Jan 1976.

13. Hirt, C.W., and Nichols, B.D.,"Volume of Fluid (VOF) Methods for the Dynamics of Free Boundaries", *Journal of Computational Physics*, Vol. 39, pp. 201 - 205, 1981.

14. Nichols, B.D., Hirt, C.W., and Hotchkiss, R.S., "SOLA-VOF: A Solution Algorithm for Transient Fluid Flow with Multiple Free Boundaries", *Los Alamos Scientific Laboratory Report LA-8355*, 121 pages, August 1980.

15. Bridges, T. J., "A Numerical Simulation of Large Amplitude Sloshing", *Proceedings of the Third International Conference on Numerical Ship Hydrodynamics*, Paris, pp. 269-284, 1981.

16. Su, T., and Kang, S.-Y., "Analysis and Testing of the Large Amplitude Liquid Sloshing in Rectangular Containers", *Seismic Engineering for Piping Systems, Tanks, and Power Plant Equipment, Pressure Vessels and Piping Conference and Exhibition*, Chicago, Illinois, ASME P.V.P. Division., pp.149-154, 1986.

17. Su, T., "Sloshing Due to Acceleration in the Rectangular Tanks", *Fluid-Structure Vibration and Liquid Sloshing, Pressure Vessels and Piping Conference*, San Diego, California., ASME P.V.P. Division, pp. 67-69 , 1987.

18. Arai, M., "Experimental and Numerical Studies of Sloshing in Liquid Cargo Tanks with Internal Structures", *IHI Engineering Review*, Vol.19, No.2, pp. 51-56, Apr. 1986.

19. Cordonnier, J.-P. V., "Numerical Simulation of Sloshing in Tanks", *Marine Offshore and Ice Technology* , Computational Mechanics Publications, pp. 197-204, 1994.

20. Arai, M., Cheng, L.Y., Inoue, Y., Sasaki,H., and Yamagishi,N., "Numerical Analysis of Liquid Sloshing in Tanks of FPSO",*Proceedings of the 2nd (1992) International Offshore and Polar Engineering Conference*, ISOPE, pp. 383-390, 1992.

21. Popov, G., Sankar, S., Sankar, T.S., and Vatistas, G.H., "Liquid Sloshing in Rectangular Road Containers", *Computers Fluids*, Vol. 21, No. 4, pp.551-569, 1992.

22. Popov, G., Vatistas, G.H., Sankar, S., and Sankar, T.S., "Dynamics of Liquid Motion in a Partially Filled Rectangular Container", *Proceedings of the 1987 ASME Computers in Engineering Conference and Exhibition*, ASME, New York, pp. 257-261, 1987

23. Popov, G., Sankar, S., Sankar, T.S., and Vatistas, G.H., "Dynamics of Liquid Sloshing in Horizontal Cylindrical Road Containers", *Proceedings of the Institute of Mechanical Engineers*, Part C, Vol. 207, pp. 399-406, 1993.

24. Abdullah, Z., and Salcudean, M., "Free Surface Flow During the Filling of a Cylinder", *International Journal for Numerical Methods in Fluids*, Vol. 11, pp. 151-168, 1990.

25. Partom, I. S., "Application of the VOF Method to the Sloshing of a Fluid in a Partially Filled Cylindrical Container", *International Journal for Numerical Methods in Fluids*, Vol. 7, pp. 535-550, 1988.

26. Huerta, A., and Liu, W.K., "Viscous Flow with Large Free Surface Motion", *Computer Methods in Applied Mechanics and Engineering*, Vol. 69, pp 277-324, 1988.

27. Ramaswamy, B., and Kawahara, M., "Lagrangian Finite Element Analysis Applied to Viscous Free Surface Fluid Flow", *International Journal for Numerical Methods in Fluids*, Vol. 7, pp. 953-984, 1987.

28. Ramaswamy, B.,and Kawahara, M., "Arbitrary Lagrangian-Eulerian Finite Element Method for Unsteady, Convective, Incompressible Viscous Free Surface Fluid Flow", *International Journal for Numerical Methods in Fluids*, Vol. 7, pp. 1053-1075, 1987.

29. Ramaswamy, B., and Kawahara, M., "Lagrangian Finite Element Method for the Analysis of Two-Dimensional Sloshing Problems", *International Journal for Numerical Methods in Fluids*, Vol. 6, pp. 659-670, 1986.

30. Patankar, S.V., *Numerical Heat Transfer and Fluid Flow*, Hemisphere Publishing Company, New York, 1980.

31. Currie, I. G., *Fundamental Mechanics of Fluids*, McGraw-Hill Inc. 1993.

32. Newman, J.N., *Marine Hydrodynamics*, The Massachusetts Institute of Technology Press, U.S.A., 1977.

Figures

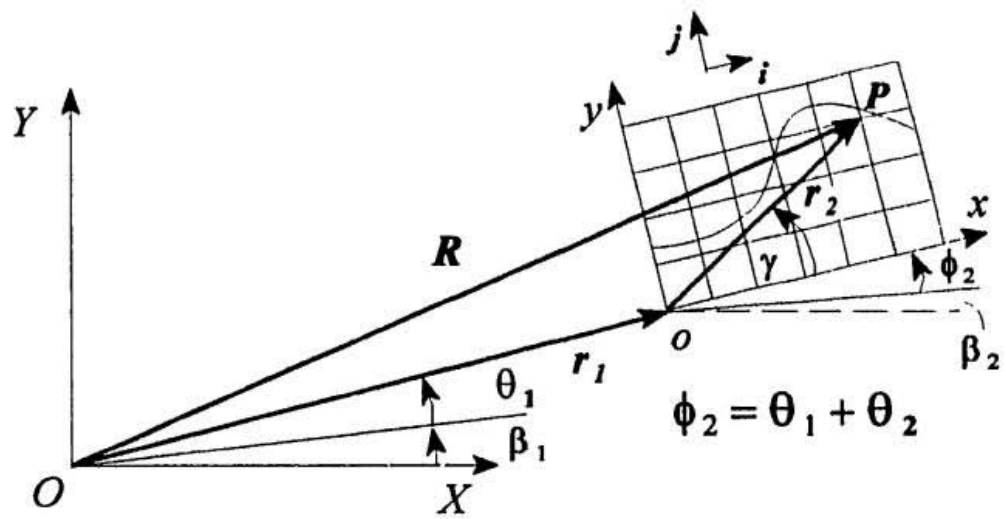

Figure 2-1
Co-ordinate Systems

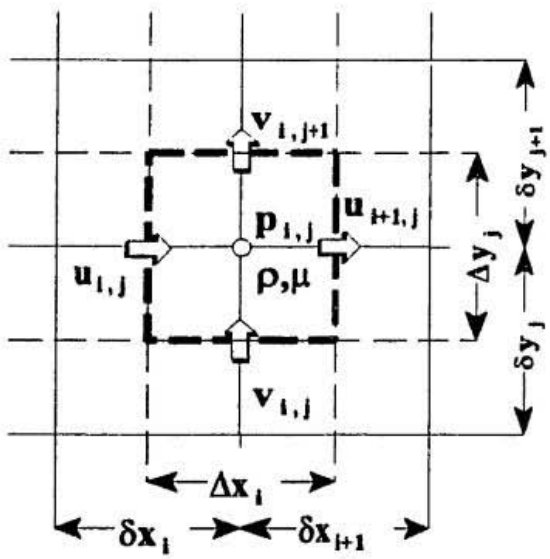

Figure 2-2
Domain Discretization Details

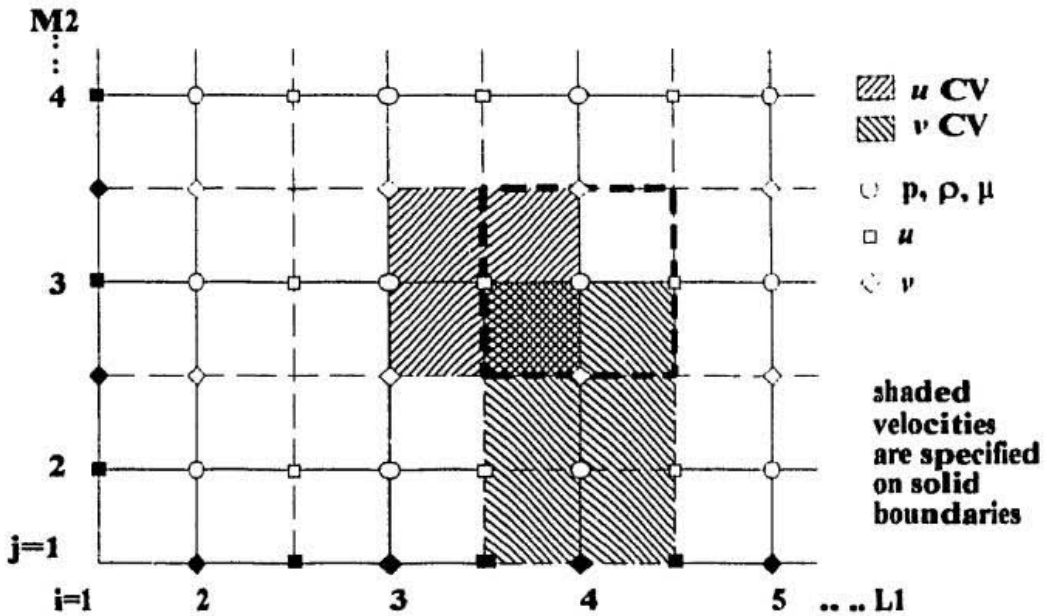

Figure 2-3
Staggered Grid Control Volumes

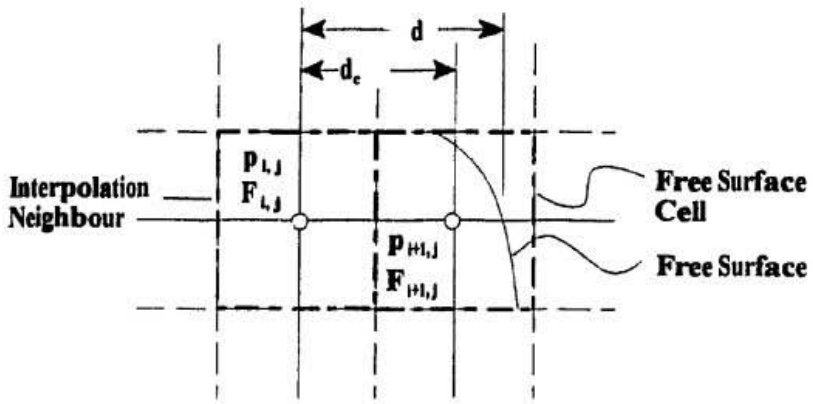

Figure 2-4
Interpolation Neighbour Cells

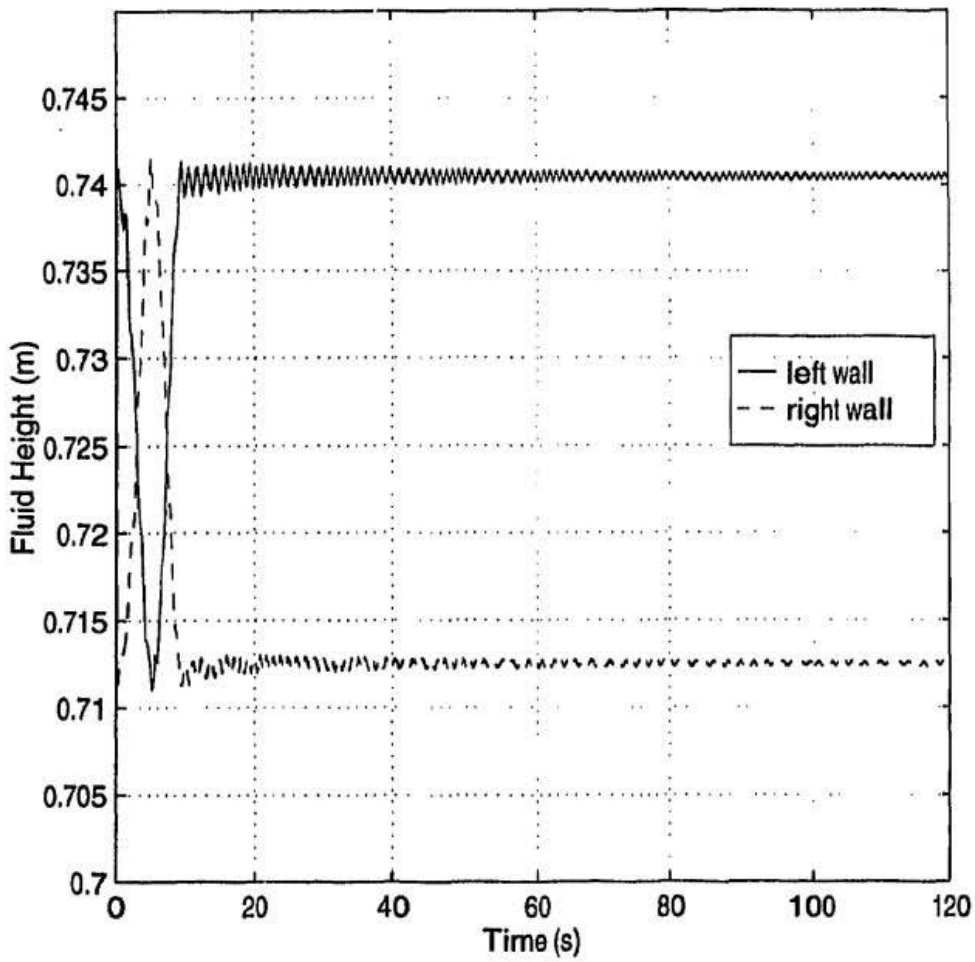

Figure 3-1
Fluid Heights at Left and Right Walls for Tank Rotation to $\beta_2 = 2.0°$ and $\theta_2 = 0°$.

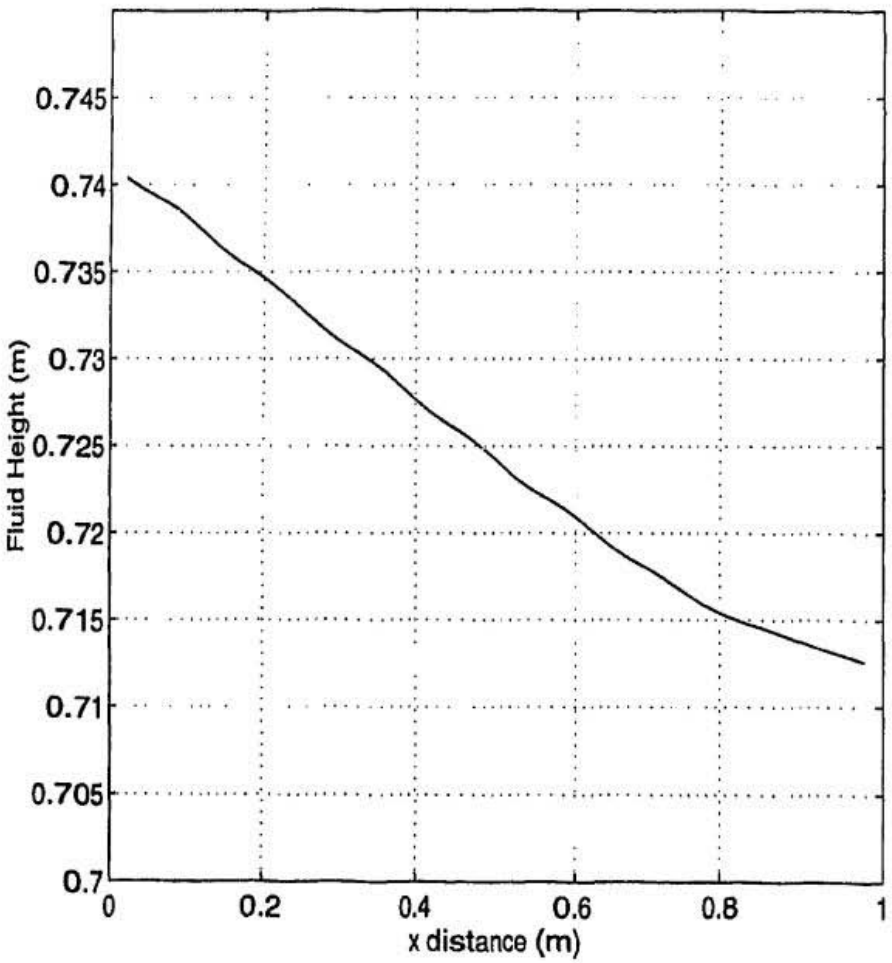

Figure 3-2
Free Surface after 120. s for Tank Rotation to $\beta_2 = 2.0°$ and $\beta_3 = 0°$.

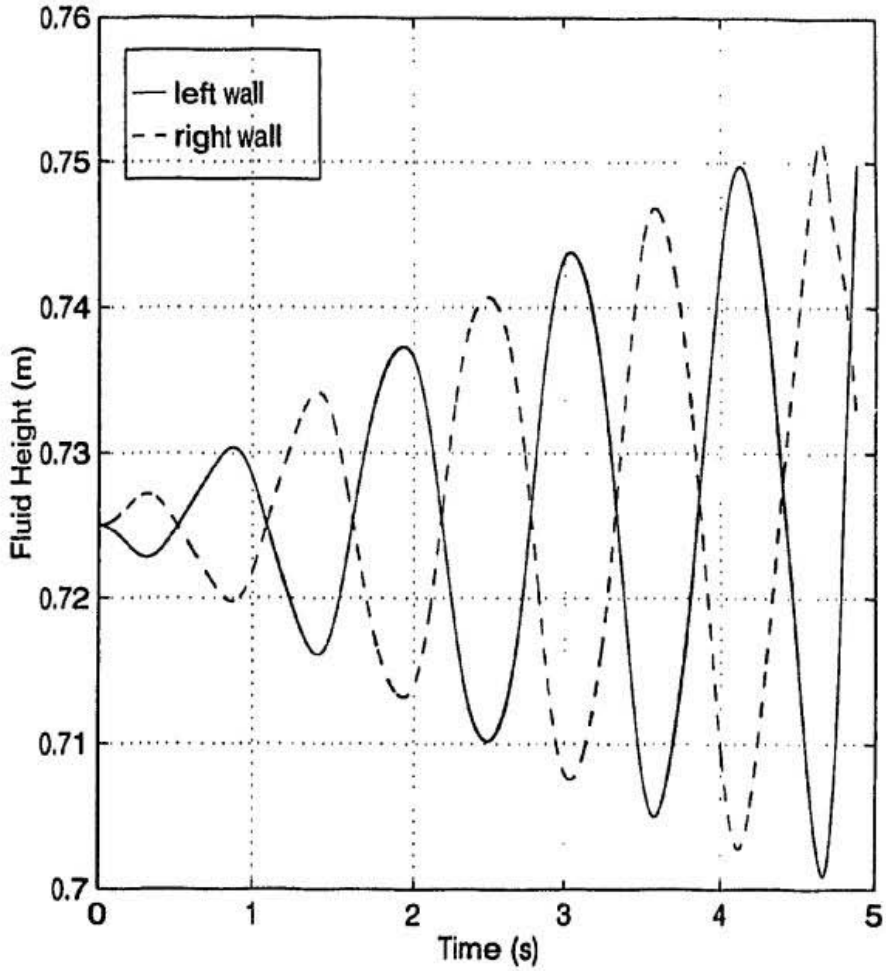

Figure 3-3
Fluid Heights at Left and Right Walls for Tank Translation at Natural Period.

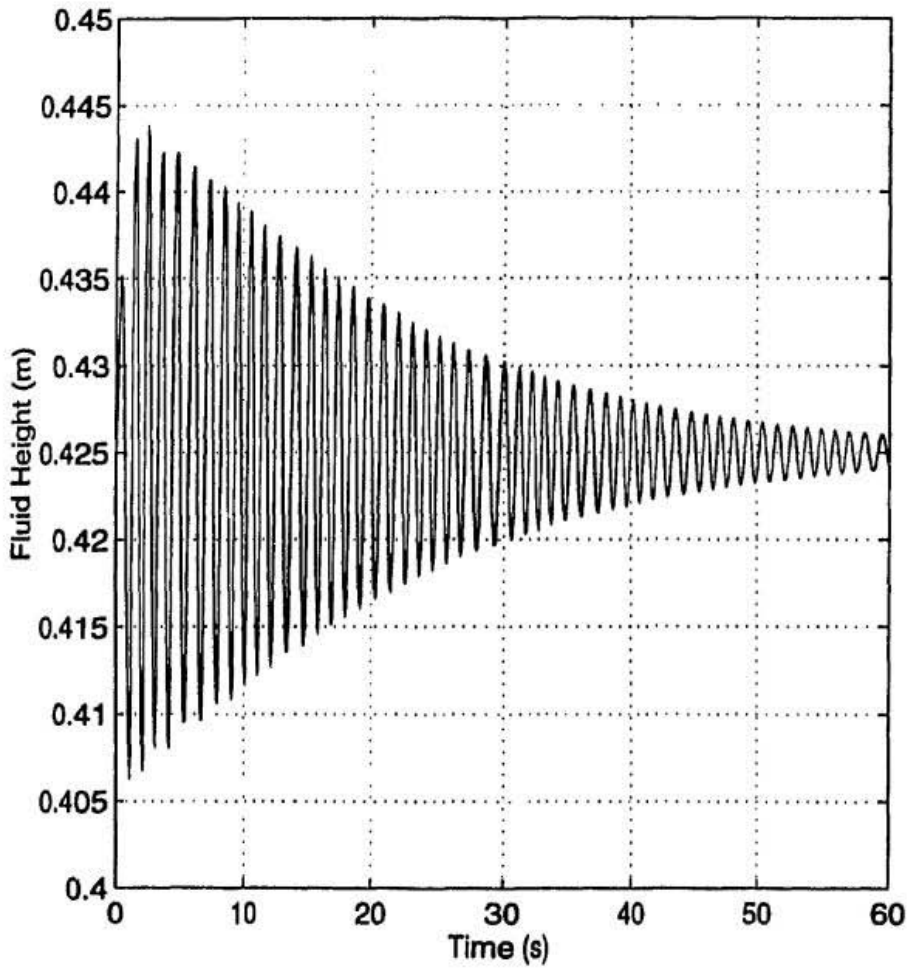

Figure 3-4
Fluid Heights at the Right Wall for Impulsive Tank Translation.

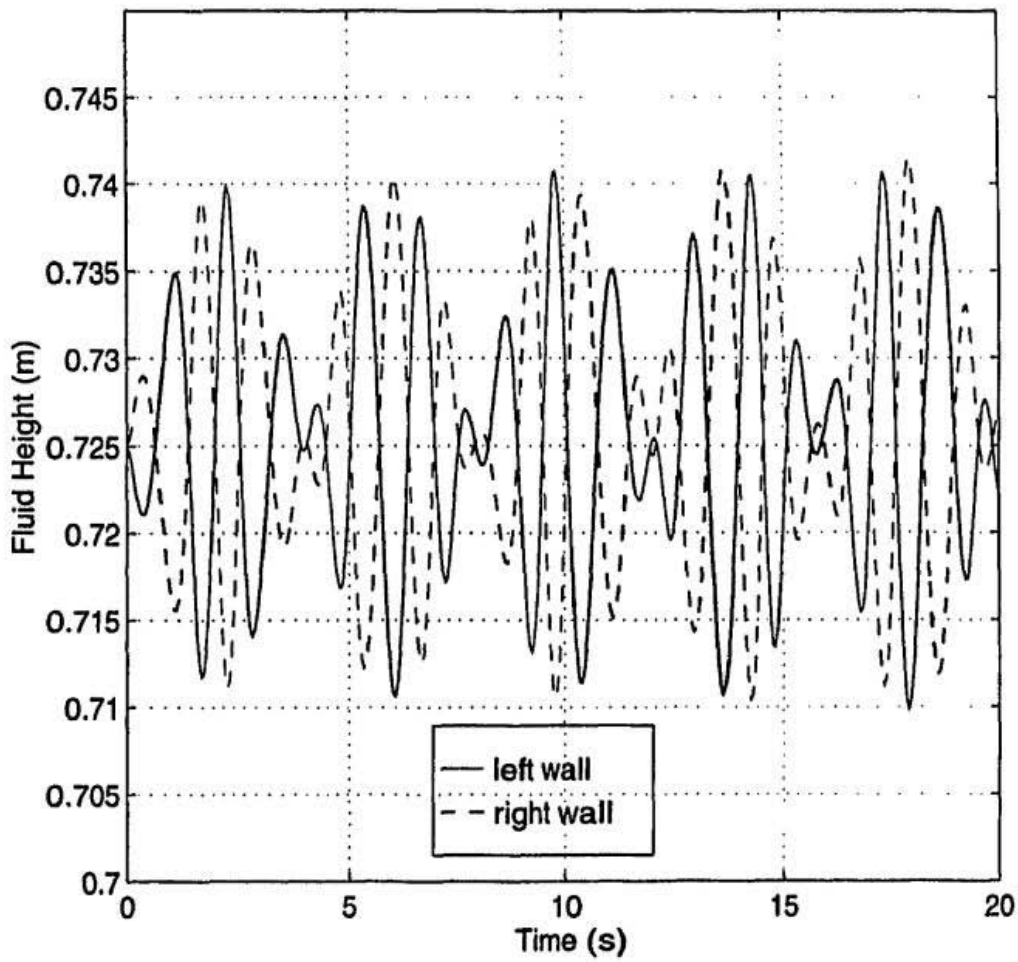

Figure 3-5
Fluid Heights at Left and Right Walls for Tank Translation with a Period Near the Natural Period.

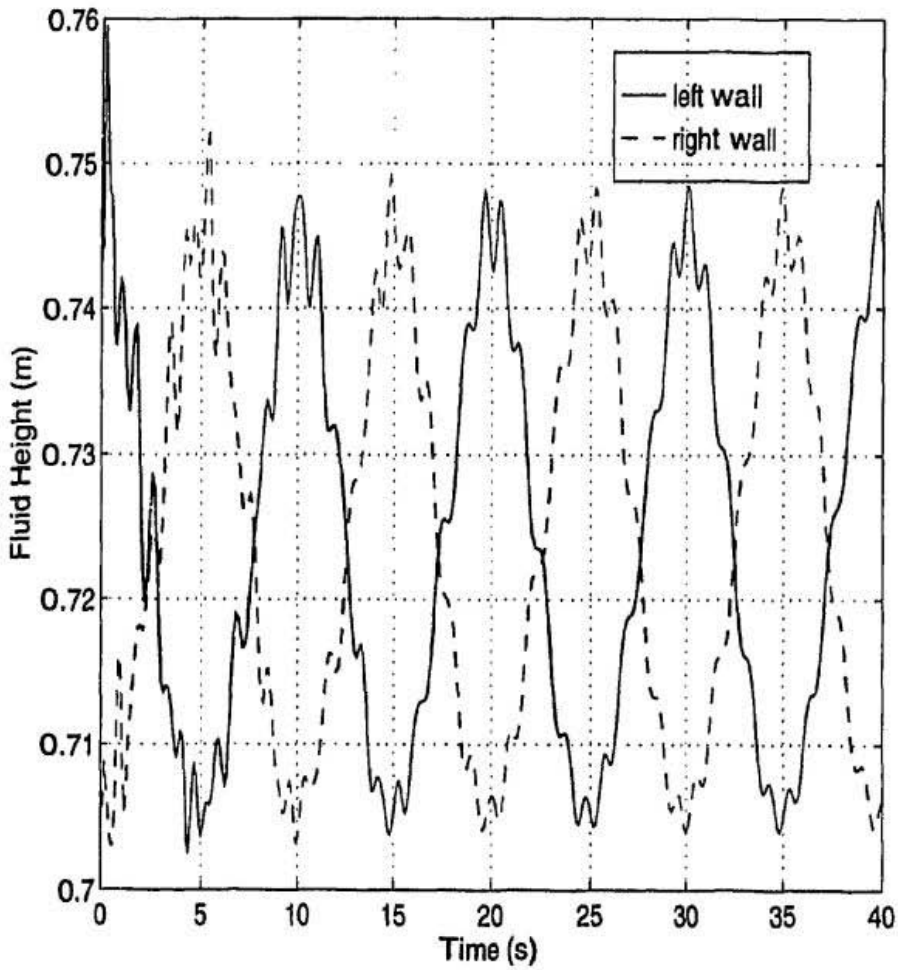

Figure 3-6
Fluid Heights at Left and Right Walls with Tank Rotation.

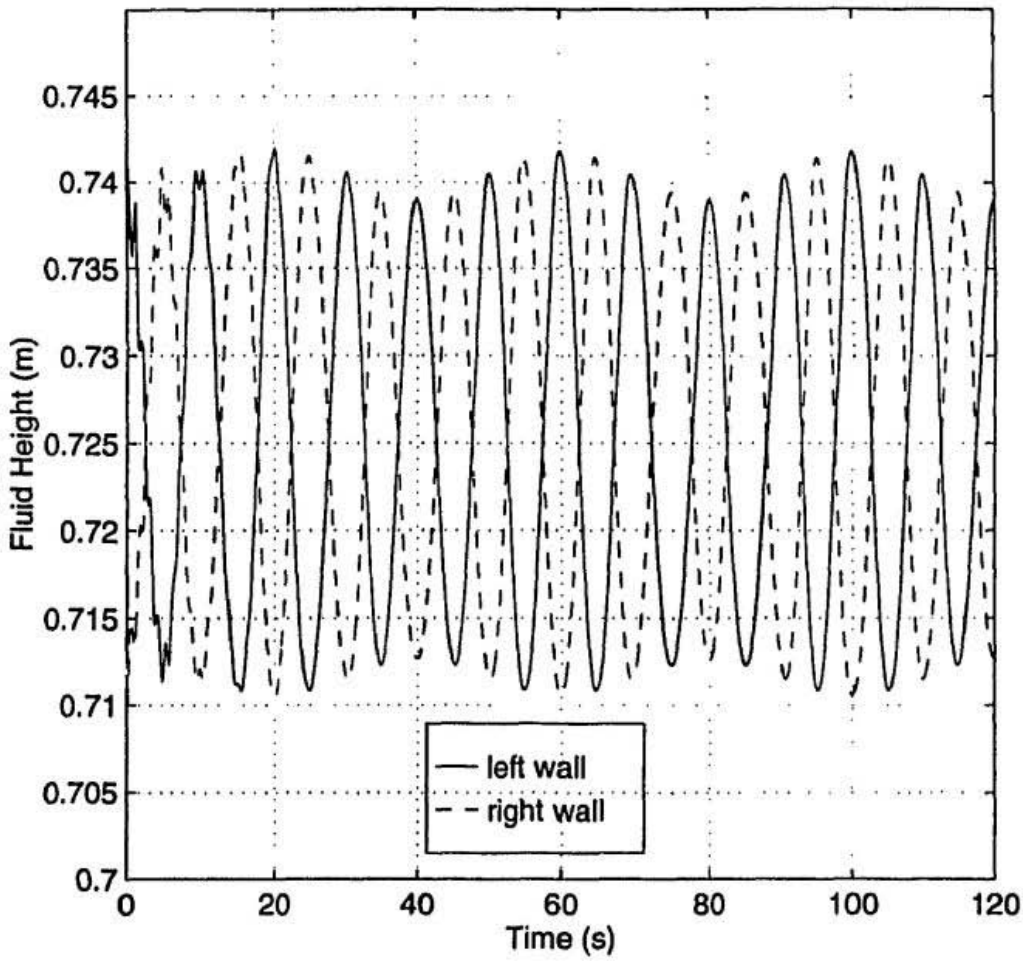

Figure 3-7
Fluid Heights at Left and Right Walls with Combined Tank Rotation and Translation.

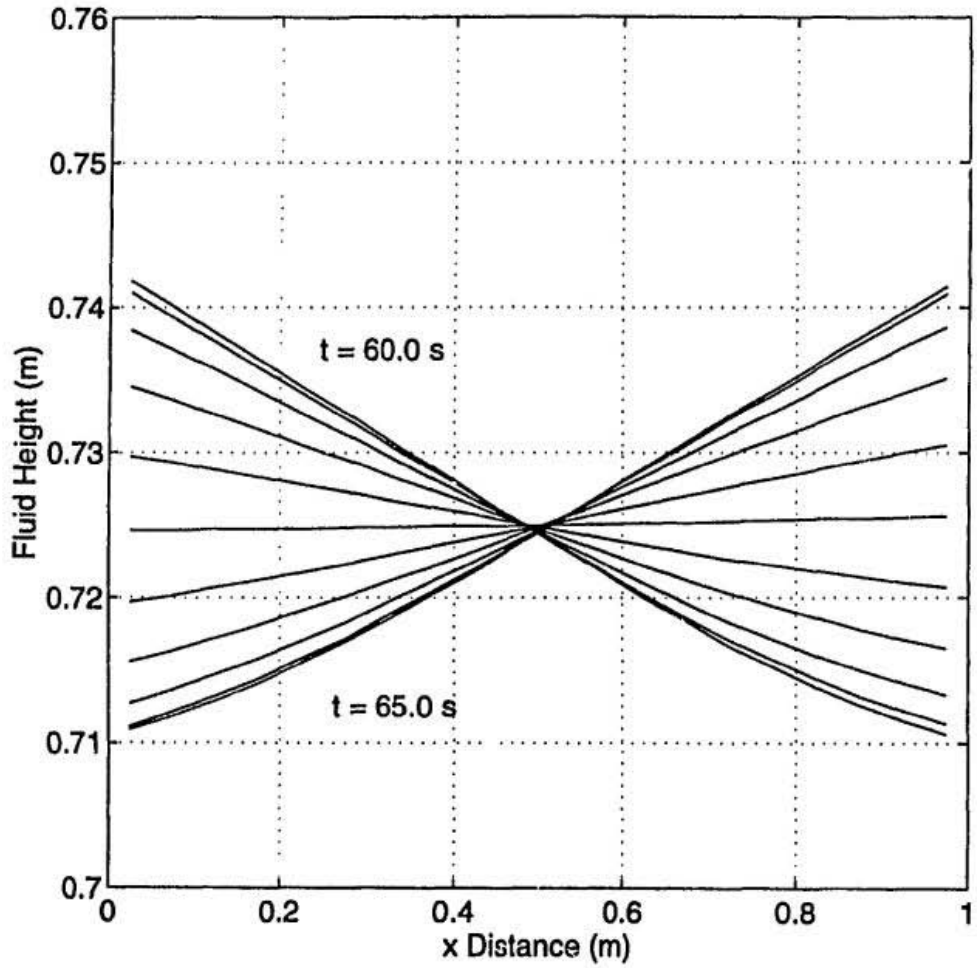

Figure 3-8
Free Surface at 0.5 s Intervals for the Timespan from 60.0 s to 65.0 s with Combined Tank Rotation and Translation.

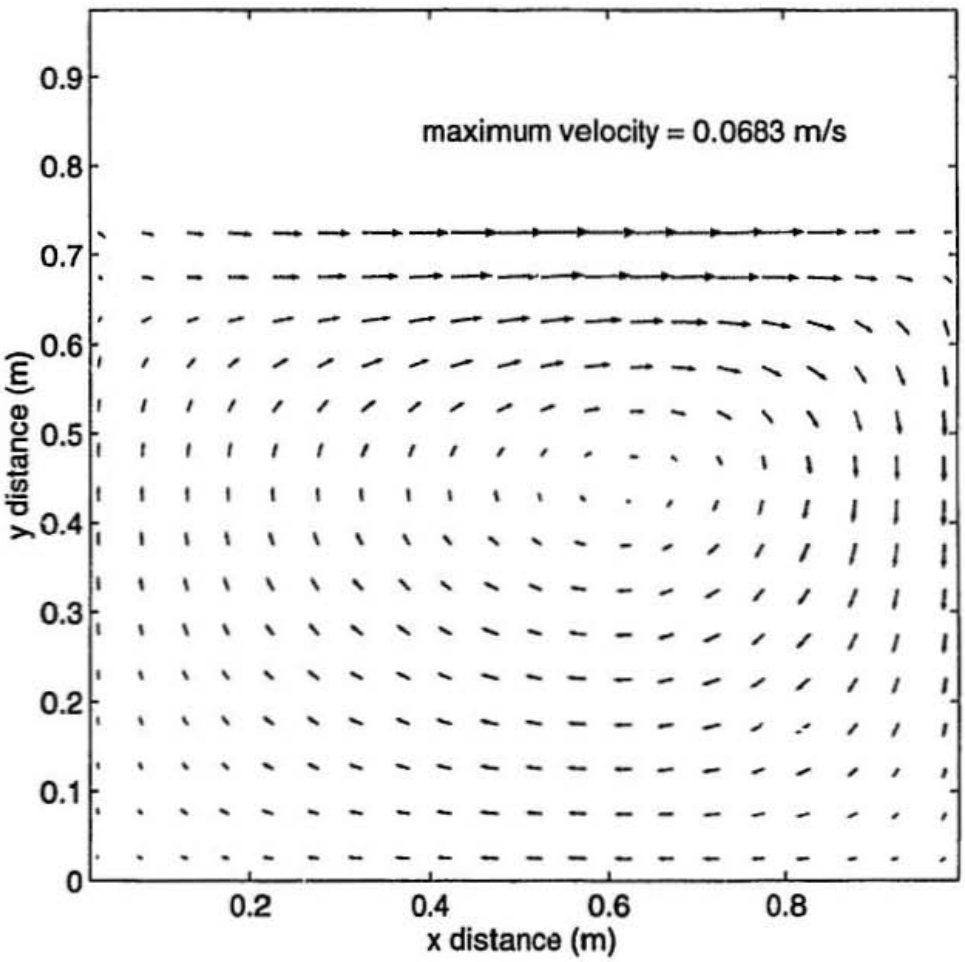

Figure 3-9
Velocity Vectors at t = 62.5 s with Combined Tank Rotation and Translation.

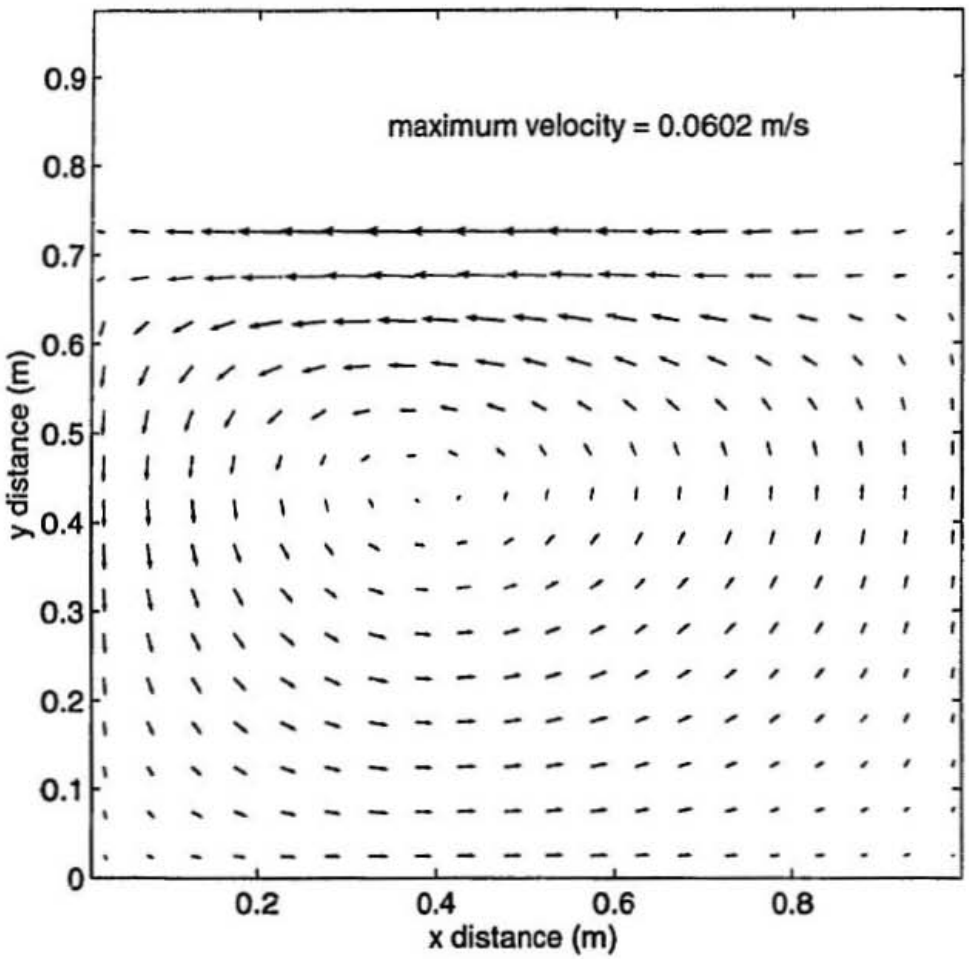

Figure 3-10
Velocity Vectors at $t = 67.5$ s with Combined Translation and Rotation.